

# Unraveling Environmental Effects on Hydrogen-Bonded Complexes: Matrix Effects on the Structures and Proton-Stretching Frequencies of Hydrogen–Halide Complexes with Ammonia and Trimethylamine

Meredith J. T. Jordan<sup>†</sup> and Janet E. Del Bene<sup>\*‡</sup>

Contribution from the School of Chemistry, University of Sydney, Sydney, NSW 2006, Australia, and Department of Chemistry, Youngstown State University, Youngstown, Ohio 44555

Received November 11, 1999. Revised Manuscript Received January 3, 2000

**Abstract:** Anharmonicity and matrix effects play important roles in determining the proton-stretching frequencies in hydrogen-bonded complexes of HCl and HBr with NH<sub>3</sub> and N(CH<sub>3</sub>)<sub>3</sub>. These effects have been investigated through ab initio calculations carried out at MP2/aug'-cc-pVDZ for complexes with HCl and at MP2/6-31+G-(d,p) for complexes with HBr. The potential surfaces of these complexes are very anharmonic, since the region surrounding the global minimum may be very broad and relatively flat, or a second region of the surface, displaced from the global minimum, can be accessed in either the ground ( $\nu = 0$ ) or the first excited ( $\nu = 1$ ) state of the proton-stretching mode. As a result, two-dimensional anharmonic frequencies, particularly for the proton-stretching vibration, can be dramatically different from the corresponding harmonic frequencies. Moreover, the zero-point energy contribution to binding enthalpies based on harmonic vibrational frequencies can be significantly overestimated in some complexes. To model the effects of matrices on the structures and spectra of these complexes, potential surfaces have been generated in the presence of external electric fields applied along the hydrogen-bonding X–H–N direction. These fields preferentially stabilize more polar hydrogen-bonded structures. The changes in anharmonic frequencies computed from these surfaces depend on the strength of the field and the nature of the equilibrium structure at zero field. Comparisons between computed frequencies for these complexes and experimental frequencies obtained in Ar and N<sub>2</sub> matrices provide insight into the dependence of proton-stretching frequencies on the environment. It is now possible to understand the apparently disparate effects of Ar and N<sub>2</sub> matrices on the spectra of closely related complexes.

## Introduction

Hydrogen bonding is one of the most important of all intermolecular interactions. It is ubiquitous in nature, giving water its unique properties, and playing a key role in the chemistry of living systems. The hydrogen bond arises when a hydrogen atom that is covalently bonded to an electronegative atom (A) in one molecule interacts with an electron-rich center (B) in another molecule, giving rise to a traditional A–H···B hydrogen bond. In this situation, the A–H distance is slightly elongated relative to the A–H distance in the corresponding monomer, and the B–H distance is significantly longer than a normal B–H covalent bond distance. A second type of hydrogen bond has been described as a proton-shared hydrogen bond,<sup>1</sup> represented as A···H···B. In this type of bond, the A–H and B–H distances are long relative to monomer distances, but the A–B distance is significantly shorter than the A–B distance in a traditional hydrogen bond. Proton-shared hydrogen bonds may be related to what have been described as short-strong hydrogen bonds (SSHBs) or low-barrier hydrogen bonds (LBHBs), which may play an important role in enzyme-catalyzed reactions. There is, however, no direct experimental evidence

that this is the case, and the role of such hydrogen bonds in enzyme catalysis is controversial.<sup>2–8</sup>

We have previously examined a number of related hydrogen-bonded complexes which are stabilized by traditional and proton-shared hydrogen bonds.<sup>9–12</sup> In this paper we further investigate the nature of such hydrogen bonds, and demonstrate how these may be stabilized in the presence of an isotropic electric field. Some experimental vibrational spectroscopic data for hydrogen-bonded complexes have been obtained in the gas phase, but more typically these data are obtained using low-temperature matrix isolation spectroscopy. It is apparent that the presence of matrix material can affect both the structure and the spectroscopy of a complex.

Our first attempt to model such interactions was to explicitly include rare gas atoms around hydrogen-bonded complexes.<sup>9,10,13</sup>

- (3) Cleland, W. W.; Kreevoy, M. M. *Science* **1994**, *264*, 1927.
- (4) Marimanikkuppam, S. S.; Lee, I.-S. H.; Binder, D. A.; Young, V. G.; Kreevoy, M. M. *Croat. Chem. Acta* **1996**, *69*, 1661.
- (5) Cleland, W. W. *Biochemistry* **1992**, *31*, 317.
- (6) Guthrie, J. P.; Kluger, R. *J. Am. Chem. Soc.* **1993**, *115*, 11569.
- (7) Guthrie, J. P. *Chem. Biol.* **1996**, *3*, 163.
- (8) Wesolowski, T.; Muller, R. P.; Warshel, A. *J. Phys. Chem.* **1996**, *100*, 15444.
- (9) Del Bene, J. E.; Jordan, M. J. T. *J. Chem. Phys.* **1998**, *108*, 3205.
- (10) Del Bene, J. E.; Jordan, M. J. T.; Gill, P. M. W.; Buckingham, A. D. *Mol. Phys.* **1997**, *92*, 429.
- (11) Del Bene, J. E.; Person, W. B.; Szczepaniak, K. *Chem. Phys. Lett.* **1995**, *247*, 89.
- (12) Del Bene, J. E.; Person, W. B.; Szczepaniak, K. *Mol. Phys.* **1996**, *89*, 47.
- (13) Del Bene, J. E.; Szczepaniak, K.; Chabrier, P.; Person, W. B. *Chem. Phys. Lett.* **1997**, *264*, 109.

<sup>†</sup> University of Sydney.

<sup>‡</sup> Youngstown State University.

(1) Del Bene, J. E. Hydrogen Bonding: 1. In *The Encyclopedia of Computational Chemistry*; Schleyer, P. v. R., Allinger, N. L., Clark, T., Gasteiger, J., Kollman, P. A., Schaefer, H. F., III, Schreiner, P. R., Eds.; John Wiley & Sons: Chichester, UK, 1998; Vol. 2, pp 1263–1271.

(2) Gerlt, J. A.; Kreevoy, M. M.; Cleland, W. W.; Frey, P. A. *Chem. Biol.* **1977**, *4*, 259.

In this present work our approach is to place a hydrogen-bonded complex in a small external electric field. Such an approach is consistent with Onsager's model for dipolar fluids.<sup>14</sup> The model used by Onsager was originally proposed by Bell<sup>15</sup> and places a point dipole,  $\mu$ , in the center of a spherical cavity within a continuous dielectric medium of relative permittivity  $\epsilon$ . The field of the dipole,  $\mu$ , polarizes its surroundings and this polarization induces a homogeneous field in the cavity, the reaction field,  $\mathbf{R}$ . If the cavity is spherical,  $\mathbf{R}$  has the same direction as  $\mu$ . The magnitude of  $\mathbf{R}$  can be calculated from the dipole moment, the cavity radius, and the relative permittivity of the dielectric medium. We assume the reaction field,  $\mathbf{R}$ , is isotropic and we calculate potential energy surfaces for a range of field strengths consistent with Onsager's model. Although a simplification, this approach provides insight into the nature and mechanism by which interaction between the complex and a matrix occurs.

In this paper we report the dependence of the structures and proton-stretching vibrational frequencies of complexes between the hydrogen halides (HCl and HBr) and ammonia (NH<sub>3</sub>) and trimethylamine [N(CH<sub>3</sub>)<sub>3</sub>] on external electric fields of varying strengths.

## Methods

The structures of all complexes have been optimized at zero field under the constraint of C<sub>3v</sub> symmetry using second-order many body Møller–Plesset perturbation theory (MP2).<sup>16–19</sup> Complexes with HBr were studied using the 6-31+G(d,p) basis set.<sup>20–23</sup> Complexes with HCl were investigated using the Dunning correlation-consistent polarized valence double-split basis set augmented with diffuse s, p, and d functions on non-hydrogen atoms (aug'-cc-pVDZ).<sup>24–26</sup> This basis was found to give an improved description of the harmonic and anharmonic vibrational frequencies of HCl relative to 6-31+G(d,p).<sup>9</sup> Vibrational frequencies were computed for all structures to identify minima, to simulate the harmonic vibrational spectra, and to obtain the zero-point vibrational energy contributions to binding enthalpies at 10 K ( $\Delta H_0^{10}$ ), the temperature at which matrix isolation measurements are made. The subscript h is used to denote that the zero-point energy correction has been evaluated exclusively from harmonic frequencies, as is usually done. However, since the potential surface describing the proton-stretching vibration can be very anharmonic, using the harmonic zero-point energy for this mode may lead to a relatively large error. To estimate the magnitude of this error, we have substituted the anharmonic zero-point vibrational energies obtained from the zero-field two-dimensional surfaces for the corresponding harmonic zero-point energies for the dimer- and proton-stretching vibrations, and have used the anharmonic zero-point energy for the monomers HCl and HBr.<sup>9</sup> The resulting binding enthalpy at 10 K will be denoted  $\Delta H_a^{10}$ .

All calculations were done freezing the s and p electrons below the valence shells in the Hartree–Fock molecular orbitals. The levels of theory used produce reliable structures and vibrational frequency shifts

- (14) Onsager, L. *J. Am. Chem. Soc.* **1936**, 58, 1486.  
 (15) Bell, R. P. *Trans. Faraday Soc.* **1931**, 27, 797.  
 (16) Pople, J. A.; Binkley, J. S.; Seeger, R. *Int. J. Quantum Chem. Quantum Chem. Symp.* **1976**, 10, 1.  
 (17) Krishnan, R.; Pople, J. A. *Int. J. Quantum Chem.* **1978**, 14, 91.  
 (18) Bartlett, R. J.; Silver, D. M. *J. Chem. Phys.* **1975**, 62, 3258.  
 (19) Bartlett, R. J.; Purvis, G. D. *Int. J. Quantum Chem.* **1978**, 14, 561.  
 (20) Hehre, W. J.; Ditchfield, R.; Pople, J. A. *J. Chem. Phys.* **1972**, 56, 2257.  
 (21) Hariharan, P. C.; Pople, J. A. *Theor. Chim. Acta* **1973**, 28, 213.  
 (22) Spitznagel, G. W.; Clark, T.; Chandrasekhar, J.; Schleyer, P. v. R. *J. Comput. Chem.* **1983**, 3, 3633.  
 (23) Clark, T.; Chandrasekhar, J.; Spitznagel, G. W.; Schleyer, P. v. R. *J. Comput. Chem.* **1983**, 4, 294.  
 (24) Dunning, T. H., Jr. *J. Chem. Phys.* **1989**, 90, 1007.  
 (25) Kendall, R. A.; Dunning, T. H., Jr.; Harrison, R. J. *J. Chem. Phys.* **1992**, 96, 1358.  
 (26) Woon, D. E.; Dunning, T. H., Jr. *J. Chem. Phys.* **1993**, 98, 1358.  
 (27) Del Bene, J. E.; Shavitt, I. In *Molecular Interactions: From Van der Waals to Strongly Bound Complexes*; Scheiner, S., Ed.; John Wiley and Sons: Sussex, 1997; pp 157–179.

**Table 1.** Configuration Space Spanned by ab Initio Data Points<sup>a</sup>

complex	field (au)	$R_{12} = \text{X-N}$ (Å)	$R_2 = \text{X-H}$ (Å)
ClH:NH <sub>3</sub> <sup>b</sup>	0.0000	$2.70 \leq R_{12} \leq 3.30$	$1.10 \leq R_2 \leq 1.70$ at $R_{12} = 2.70$ to $1.10 \leq R_2 \leq 2.30$ at $R_{12} = 3.30$
	0.0010		
	0.0025		
	0.0040		
	0.0055		
	0.0100		
	0.0150		
BrH:NH <sub>3</sub> <sup>c</sup>	0.0000	$2.80 \leq R_{12} \leq 3.50$	$1.20 \leq R_2 \leq 1.80$ at $R_{12} = 2.80$ to $1.20 \leq R_2 \leq 2.50$ at $R_{12} = 3.50$
	0.0005		
	0.0010		
	0.0025	$2.70 \leq R_{12} \leq 3.50$	$1.10 \leq R_2 \leq 1.85$ at $R_{12} = 2.70$ to $1.10 \leq R_2 \leq 2.65$ at $R_{12} = 3.50$
	0.0040		
	0.0080		
	0.0005		
	0.0010		
	0.0025		
	0.0040		
ClH:N(CH <sub>3</sub> ) <sub>3</sub>	0.0000	$2.50 \leq R_{12} \leq 3.50$	$1.10 \leq R_2 \leq 1.60$ at $R_{12} = 2.50$ to $1.10 \leq R_2 \leq 2.60$ at $R_{12} = 3.50$
	0.0010		
	0.0040		
BrH:N(CH <sub>3</sub> ) <sub>3</sub>	0.0000	$2.50 \leq R_{12} \leq 3.40$	$1.10 \leq R_2 \leq 1.60$ at $R_{12} = 2.50$ to $1.10 \leq R_2 \leq 2.50$ at $R_{12} = 3.40$
	0.0010		
	0.0040		

<sup>a</sup> Points were calculated at 0.05 Å increments unless otherwise specified. <sup>b</sup> For ClH:NH<sub>3</sub> at 0.0055 au, field ab initio points were not obtained at coordinates ( $R_1, R_2$ ) = (1.00, 2.00), (1.00, 2.05), (1.00, 2.10), (1.05, 1.95), (1.05, 2.00), and (1.05, 2.05). <sup>c</sup> For BrH:NH<sub>3</sub> no ab initio data were obtained for the Br–N distance 3.35 Å at field strengths of 0.0080 and 0.0120 au, and no ab initio data were obtained for any field strength considered for Br–N = 3.45 Å.

for the proton-stretching band relative to the monomer if the anharmonicity correction in the complex is not large, and reasonable binding energies.<sup>1,27–29</sup> However, the computed MP2 binding energies for all of these complexes are too large, since neither the wave function model (MP2) nor the basis set used yield near converged values. For example, the binding energies for ClH:NH<sub>3</sub> at MP2/aug'-cc-pVDZ, MP2/aug'-cc-pVTZ, and CCSD(T)/aug'-cc-pVTZ are -9.5, -9.0, and -8.1 kcal/mol, respectively. The difference due to the wave function model, which can be seen by comparing the MP2/aug'-cc-pVTZ and CCSD(T)/aug'-cc-pVTZ energies, is greater than the difference due to the basis set, as seen by comparing the MP2/aug'-cc-pVDZ and MP2/aug'-cc-pVTZ energies. Computing binding energies from counterpoise corrected<sup>30</sup> MP2/aug'-cc-pVDZ energies does not lead to improved energies, since it has been observed that uncorrected aug'-cc-pVXZ energies converge faster and are closer to basis-set converged values than counterpoise-corrected aug'-cc-pVXZ energies.<sup>1,27</sup> The objective of the present study is not to provide quantitatively accurate binding energies, but to show how potential surfaces obtained at a reasonable level of theory change with external field strength, and how the variation in structural and vibrational spectroscopic properties parallel these changes.

The two-dimensional potential energy surfaces were generated by freezing the ammonia or trimethylamine coordinates, similarly to earlier work,<sup>9,10</sup> and then varying the N–H and X–H distances. Results at nonzero field strengths were similarly obtained by applying an external field along the X–H–N direction of the complex and varying the N–H and X–H distances. In this way a discrete grid of ab initio data was obtained for each complex considered. The coordinate values used to construct the ab initio grids are given in Table 1. The ab initio data cover the most chemically relevant areas of the potential surfaces including those regions associated with traditional, proton-shared, and ion-pair hydrogen bonds, and extend sufficiently far to describe the walls of the potential energy surfaces.

Global potential energy surfaces were constructed from the ab initio data using the following procedure:

- (28) Del Bene, J. E.; Person, W. B.; Szczepaniak, K. *J. Phys. Chem.* **1995**, 99, 10705.  
 (29) Del Bene, J. E.; Jordan, M. J. T. *Int. Rev. Phys. Chem.* **1999**, 18, 119.  
 (30) Boys, S. F.; Bernardi, F. *Mol. Phys.* **1970**, 19, 553.

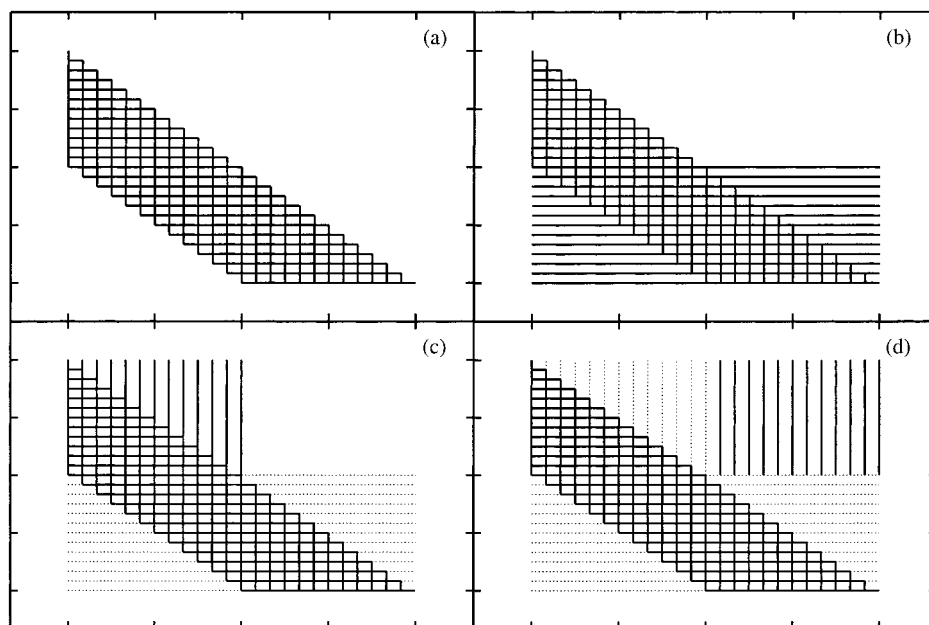


**Figure 1.** Schematic representation of the grid used to construct the potential surfaces from the ab initio data points: (a) the original ab initio data points; (b) one-dimensional quadratic extrapolation in the  $R_1$  coordinate, from the ab initio data; (c) one-dimensional linear extrapolation in the  $R_2$  coordinate, from the ab initio data; and (d) one-dimensional linear extrapolation in the  $R_2$  coordinate, from the grid formed in (b).

(1) One-dimensional quadratic extrapolations were performed along the N–H distance to obtain a rectangular grid covering the ab initio values.

(2) One-dimensional linear extrapolation was performed along the X–H distance to obtain a rectangular grid out to the longest X–H distance considered.

(3) A one-dimensional linear extrapolation in the X–H distance was performed on the grid obtained in Step 1 out to the longest X–H distance considered.

A schematic of this procedure is shown in Figure 1.

In this way an “augmented” rectangular grid of data points was obtained. A bicubic spline interpolation was used to describe the potential energy surface within this grid and polynomial extrapolation was used outside the grid. At short bond lengths a quadratic extrapolation was used and at long bond lengths the extrapolation was linear. The details of the construction of the augmented potential grid are slightly different from those described in our earlier work.<sup>9,10</sup> The computational effort involved in constructing this new grid is reduced relative to constructing a rectangular ab initio grid. The procedure outlined above was found to be robust and was effectively automated. For 7 of the 20 potential surfaces constructed, however, it was necessary to make small adjustments to extrapolated points on the edge of the augmented grid to ensure that the polynomial extrapolation used to construct the global surface maintained the correct curvature. When such manipulations were necessary, the required change in energy was of the order of a millihartree or less, and the energy of the augmented point was always significantly higher than energies accessed by any of the computed vibrational wave functions. The energies altered were, typically, 0.2 hartree above the energy of the global minimum on the surfaces. Extrapolations from the augmented grid used the same methods and parameters described previously.<sup>9,10</sup>

The resulting two-dimensional potential energy surfaces describe a pseudo-triatomic system, A–H–B, where A represents the  $\text{NH}_3$  or  $\text{N}(\text{CH}_3)_3$  moiety and B is the halogen. The bond lengths  $R_1$  and  $R_2$  are the distance from the H to the center-of-mass of A and the B–H distance, respectively. Where appropriate,  $R_1$  has been subsequently transformed back to the N–H distance. Minimum energy configurations and harmonic frequencies were obtained on the pseudo-triatomic surfaces using normal-mode analyses.

Two-dimensional vibrational eigenfunctions and eigenvalues were calculated as previously,<sup>9</sup> using a model Hamiltonian for the collinear A–H–B system in the  $R_1$  and  $R_2$  coordinates described above. Eigenfunctions were calculated variationally using the discrete variable

**Table 2.** Ab Initio Points and Two-Dimensional Anharmonic Frequencies for the Dimer (Heavy Atom) and Proton-Stretching Modes ( $\text{cm}^{-1}$ )

species	no. of points	area of config. spaced covered ( $\text{\AA}^2$ )	dimer	proton
$\text{ClH}:\text{NH}_3$				
ref 10	143	0.30	199	1566
this work	247	0.54	202	1567
$\text{BrH}:\text{NH}_3$				
ref 9	569	0.27	218	888
this work	349	0.92	210	908

representation (DVR)<sup>31</sup> of a two-dimensional basis set constructed as a direct product of one-dimensional tri-diagonal Morse functions,<sup>32</sup> each optimized to the appropriate one-dimensional Schrödinger equation. The results quoted below used either 120:60 or 140:70 primitive:contracted basis functions in each coordinate, and the vibrational eigenvalues are converged to better than  $0.5 \text{ cm}^{-1}$ .

One-dimensional eigenvectors and eigenvalues were also calculated for all complexes. These calculations were performed along either the proton- or the dimer-stretching normal mode displacement vectors, as obtained from a normal-mode analysis of the two-dimensional pseudo-triatomic potential surface. Tri-diagonal Morse basis functions were again used to expand the vibrational wave functions, and the eigenvalues are converged to better than  $0.01 \text{ cm}^{-1}$ .

The zero-field surfaces described here for  $\text{ClH}:\text{NH}_3$  and  $\text{BrH}:\text{NH}_3$  are based on more extensive ab initio data than those reported previously.<sup>9,10</sup> The differences between the current two-dimensional vibrational frequencies and our earlier work provide estimates of the errors introduced using polynomial extrapolation in generating the global potential energy surface. The current calculations are compared to our previous results in Table 2. Results for the  $\text{BrH}:\text{NH}_3$  complex are more sensitive than those for  $\text{ClH}:\text{NH}_3$  because the original ab initio data for  $\text{BrH}:\text{NH}_3$  covered a significantly smaller region of configuration space than those reported here. The  $\text{BrH}:\text{NH}_3$  potential surface is quite complex and, at the MP2/6-31+G(d,p) level of theory, has two local minima. Both minima and the small barrier between them lie below the zero-point vibrational energy. The present and our earlier attempts at a  $\text{BrH}:\text{NH}_3$  potential surface describe the minima well, but the results of Table 2 indicate that it is also important to adequately describe the

(31) Bacic, Z.; Light, J. C. *Annu. Rev. Phys. Chem.* **1989**, *40*, 469.

(32) Wei, H.; Carrington, T., Jr. *J. Chem. Phys.* **1992**, *97*, 3029.



nature of the repulsive walls. The differences observed between the two calculations for BrH:NH<sub>3</sub> are a result of the previous quadratic extrapolation underestimating the curvature of the walls. The results for ClH:NH<sub>3</sub>, however, indicate that, provided an adequate region of configuration space is spanned by the ab initio data points, polynomial extrapolation has little effect on the final calculated anharmonic frequencies. Details of the ab initio points used to define the potential energy surfaces are provided in Table 1.

The potential energy surfaces quoted in this work were constructed using linear extrapolation at "long" bond lengths and quadratic extrapolation at "short" bond lengths. The sensitivity of the calculated frequencies to the extrapolation procedure was determined by performing extrapolations at zero, first, and second orders (and all combinations) on the zero-field surfaces. Further, the procedure used to calculate the augmented grid was also varied, with linear and quadratic extrapolation considered. Third and fourth order extrapolation were not used because they often yielded incorrect curvature in the potential surface. As expected, the largest variations in calculated frequencies were obtained when zero-order extrapolations were used at both "long" and "short" bond lengths, that is, the potential surface was considered to be flat outside the augmented potential grid. This yielded estimates for the dimer- and proton-stretching frequencies that were lower by a maximum of 6 and 7 cm<sup>-1</sup>, respectively, for the four complexes considered.

All calculations reported here were carried out on the Cray T94 computer at the Ohio Supercomputer Center and on the computing facilities at the University of Cambridge and the University of Sydney. Gaussian 98<sup>33</sup> was used to optimize geometries and compute harmonic vibrational frequencies, and to generate the ab initio data points for the potential energy surfaces without and with electric fields.

## Results and Discussion

**Structural and Spectral Data for Complexes Without an External Field. (a) ClH:NH<sub>3</sub>.** From a structural point of view, the complex ClH:NH<sub>3</sub> has a traditional hydrogen bond with computed Cl–N and Cl–H distances ( $R_e$ ) of 3.080 and 1.341 Å,<sup>9</sup> respectively, as reported in Table 3. That the computed HCl distance is only slightly elongated relative to the HCl monomer distance of 1.288 Å indicates that proton transfer to N does not occur in this structure. This result is in agreement with Legon's conclusion based on his microwave study that the proton is not transferred to NH<sub>3</sub>.<sup>34</sup> The electronic binding energy ( $\Delta E_e$ ) of this complex is -9.5 kcal/mol. The zero-point vibrational energy contribution obtained from the harmonic frequencies is +1.7 kcal/mol, leading to a binding enthalpy ( $\Delta H_h^{10}$ ) of -7.8 kcal/mol. When the contributions to the zero-point energy of the complex arising from the proton- and dimer-stretching modes are replaced by anharmonic zero-point energies, and the anharmonic zero-point energy is used for HCl, the zero-point vibrational contribution is reduced by 0.2 kcal/mol, giving a new binding enthalpy ( $\Delta H_a^{10}$ ) of -8.0 kcal/mol. These data are summarized in Table 4. The small difference in the harmonic and anharmonic zero-point corrections is a result of similar energies for the  $\nu = 0$  levels of these vibrations. In the ground vibrational state, the complex is essentially constrained to the potential well surrounding the global minimum, as seen in Figure 2.

(33) Frisch, M. J.; Trucks, G. W.; Schlegel, H. B.; Scuseria, G. E.; Robb, M. A.; Cheeseman, J. R.; Zakrzewski, V. G.; Montgomery, J. A., Jr.; Stratmann, R. E.; Burant, J. C.; Dapprich, S.; Millam, J. M.; Daniels, A. D.; Kudin, K. N.; Strain, M. C.; Farkas, O.; Tomasi, J.; Barone, V.; Cossi, M.; Cammi, R.; Mennucci, B.; Pomelli, C.; Adamo, C.; Clifford, S.; Ochterski, J.; Petersson, G. A.; Ayala, P. Y.; Cui, J.; Morokuma, K.; Malick, D. K.; Rabuck, A. D.; Raghavachari, K.; Foresman, J. B.; Cioslowski, J.; Ortiz, J. V.; Baboul, A. G.; Stefanov, B. B.; Liu, G.; Liashenko, A.; Piskorz, P.; Komaromi, I.; Gomperts, R.; Martin, R. L.; Fox, D. J.; Keith, T.; Al-Laham, M. A.; Peng, C. Y.; Nanayakkara, A.; Gonzalez, C.; Challacombe, M.; Gill, P. M. W.; Johnson, B.; Chen, W.; Wong, M. W.; Andres, J. L.; Gonzalez, C.; Head-Gordon, M.; Replogle, E. S.; Pople, J. A. *Gaussian 98*; Gaussian, Inc.: Pittsburgh, PA, 1998.

(34) Legon, A. C. *Chem. Soc. Rev.* **1993**, 22, 153.

**Table 3.** Equilibrium ( $R_e$ ) and Expectation Values ( $R_0$ ) in the Ground Vibrational State of X–N and X–H Distances (Å) in XH:NH<sub>3</sub> and XH:N(CH<sub>3</sub>)<sub>3</sub> Complexes as a Function of Field Strength (au)<sup>a</sup>

ClH:NH <sub>3</sub>				
field	$R_0(\text{Cl–N})$	$R_e(\text{Cl–N})$	$R_0(\text{Cl–H})$	$R_e(\text{Cl–H})$
0.0000	3.016	3.080	1.392	1.341
0.0010	2.986	3.056	1.411	1.349
0.0025	2.941	3.019	1.448	1.363
0.0040	2.905	2.975	1.495	1.383
0.0055	2.870	2.832	1.546	1.575
0.0100	2.898	2.896	1.692	1.766
0.0150	2.988	3.004	1.857	1.917
BrH:NH <sub>3</sub>				
field	$R_0(\text{Br–N})$	$R_e(\text{Br–N})$	$R_0(\text{Br–H})$	$R_e(\text{Br–H})$
0.0000	3.053	3.247	1.623	1.462
0.0005	3.037	3.224	1.651	1.469
0.0010	3.027	2.976	1.676	1.778
0.0025	3.016	2.993	1.740	1.830
0.0040	3.021	3.009	1.794	1.868
0.0080	3.066	3.068	1.910	1.965
0.0120	3.142	3.152	2.027	2.075
ClH:N(CH <sub>3</sub> ) <sub>3</sub>				
field	$R_0(\text{Cl–N})$	$R_e(\text{Cl–N})$	$R_0(\text{Cl–H})$	$R_e(\text{Cl–H})$
0.0000	2.850	2.825	1.615	1.658
0.0010	2.855	2.836	1.640	1.685
0.0040	2.880	2.872	1.706	1.752
BrH:N(CH <sub>3</sub> ) <sub>3</sub>				
field	$R_0(\text{Br–N})$	$R_e(\text{Br–N})$	$R_0(\text{Br–H})$	$R_e(\text{Br–H})$
0.0000	2.991	2.983	1.830	1.870
0.0010	3.001	2.993	1.849	1.887
0.0040	3.032	3.027	1.904	1.937

<sup>a</sup> Based on MP2/aug'-cc-pVDZ data for HCl complexes and MP2/6-31+G(d,p) data for HBr complexes.

**Table 4.** Binding Energies ( $\Delta E_e$ ), Binding Enthalpies at 10 K ( $\Delta H_h^{10}$ ), and Zero-Point Vibrational Energy Contributions to Binding Enthalpies ( $\Delta ZPE$ ) for Complexes of HCl and HBr with NH<sub>3</sub> and N(CH<sub>3</sub>)<sub>3</sub><sup>a,b</sup>

complex	$\Delta E_e$	$\Delta ZPE_h$	$\Delta H_h^{10}$	$\Delta ZPE_a$	$\Delta H_a^{10}$
ClH:NH <sub>3</sub>	-9.5	1.7	-7.8	1.5	-8.0
BrH:NH <sub>3</sub>	-10.0	2.2	-7.8	1.4	-8.6
ClH:N(CH <sub>3</sub> ) <sub>3</sub>	-17.8	3.2	-14.6	2.6	-15.2
BrH:N(CH <sub>3</sub> ) <sub>3</sub>	-26.7	4.8	-21.9	4.6	-22.1

<sup>a</sup> Energies in kcal/mol. <sup>b</sup>  $\Delta ZPE_h$  and  $\Delta H_h^{10}$  are computed from the harmonic frequencies for the proton- and dimer-stretching vibrations;  $\Delta ZPE_a$  and  $\Delta H_a^{10}$  are computed from the anharmonic frequencies for these modes.

As shown in our previous study,<sup>9</sup> the region of the ClH:NH<sub>3</sub> potential energy surface associated with a proton-shared hydrogen bond lies sufficiently higher in energy relative to the global minimum that the ground-state vibrational wave function is localized within the potential well for the traditional hydrogen-bonded structure. However, in the  $\nu = 1$  state of the proton-stretching mode, the excited wave function is no longer localized in the potential well, but extends into the proton-shared region of the surface, as evident from Figure 3. This leads to a large anharmonicity correction for the proton-stretching frequency.

Table 5 reports harmonic and anharmonic frequencies for the proton-stretching mode. The harmonic proton-stretching frequencies obtained from the full and pseudo-triatomic surfaces are similar at 2289 and 2278 cm<sup>-1</sup>, respectively. These are reduced to 1905 cm<sup>-1</sup> in the one-dimensional anharmonic treatment, and to 1567 cm<sup>-1</sup> in the two-dimensional anharmonic

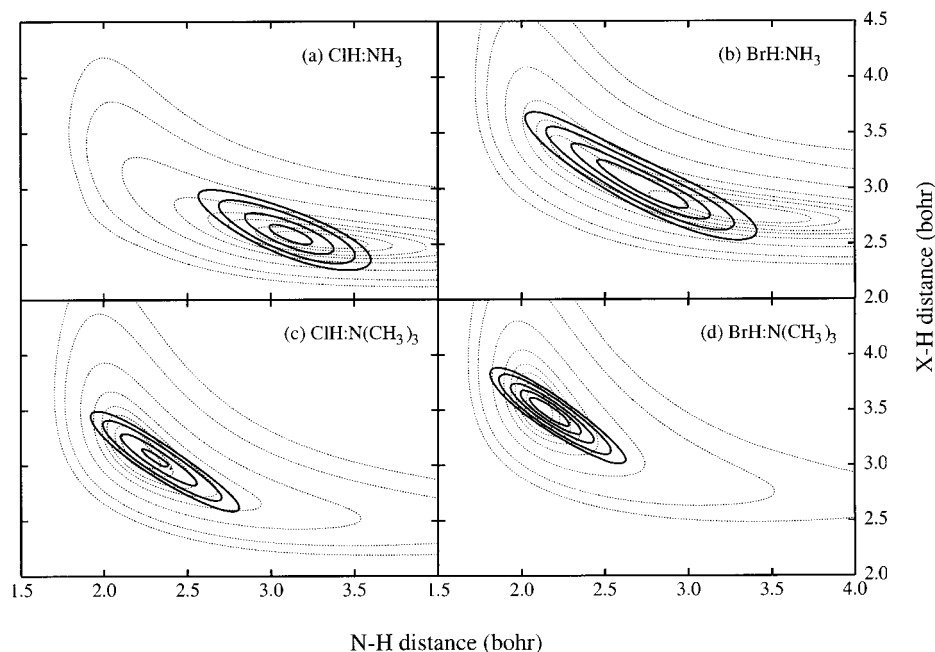


**Figure 2.** Square of the ground-state vibrational wave functions for (a) ClH:NH<sub>3</sub>, (b) BrH:NH<sub>3</sub>, (c) ClH:N(CH<sub>3</sub>)<sub>3</sub>, and (d) BrH:N(CH<sub>3</sub>)<sub>3</sub> at zero field superimposed on the potential surfaces. Contour values are at 0.0005, 0.001, 0.002, 0.003, 0.005, 0.01, 0.02, and 0.03 au above the global minimum. The same contour values appear in all figures which display potential surfaces.

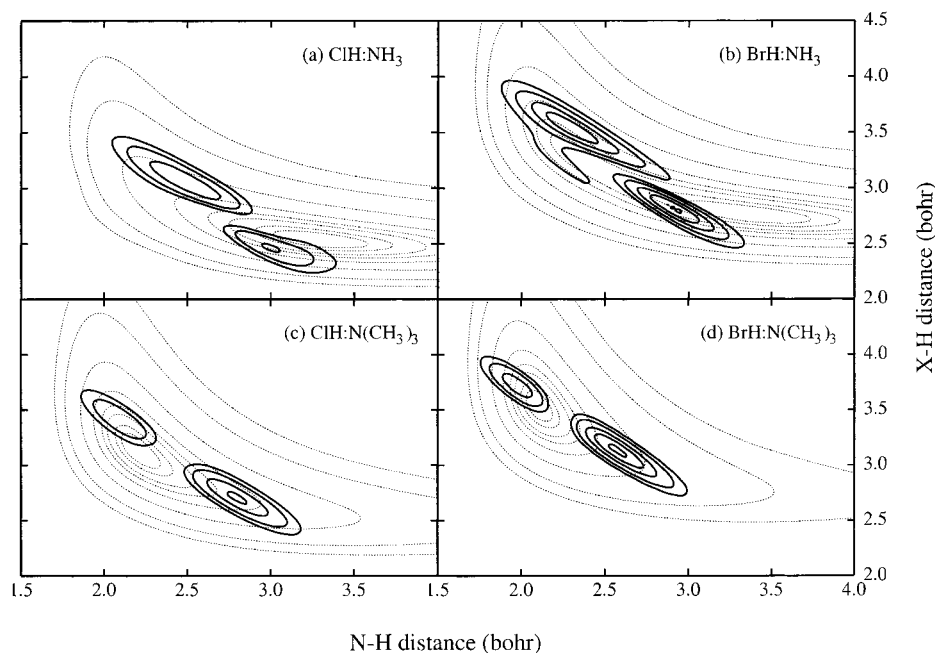


**Figure 3.** Square of the wave functions for the  $\nu = 1$  state of the proton-stretching vibration for (a) ClH:NH<sub>3</sub>, (b) BrH:NH<sub>3</sub>, (c) ClH:N(CH<sub>3</sub>)<sub>3</sub>, and (d) BrH:N(CH<sub>3</sub>)<sub>3</sub> at zero field superimposed on the potential surfaces.

treatment. The difference between the one- and two-dimensional frequencies is indicative of the importance of coupling between the proton and dimer stretching modes. The two-dimensional anharmonic frequency is significantly improved relative to the harmonic frequencies, but is still about 200 cm<sup>-1</sup> higher than the experimental frequency of 1371 cm<sup>-1</sup> in an Ar matrix which Barnes assigned to the proton-stretching vibration.<sup>35</sup> The experimentally determined frequency of the proton-stretching band of this same complex in an N<sub>2</sub> matrix is 720 cm<sup>-1</sup>.<sup>35</sup>

**(b) BrH:NH<sub>3</sub>.** The BrH:NH<sub>3</sub> complex also has a structure with a traditional hydrogen bond, with an MP2/6-31+G(d,p)

electronic binding energy of -10.0 kcal/mol and a harmonic zero-point energy contribution of 2.2 kcal/mol, leading to a binding enthalpy ( $\Delta H_h^{10}$ ) of -7.8 kcal/mol. The anharmonic zero-point vibrational energy contribution is only 1.4 kcal/mol, giving a binding enthalpy ( $\Delta H_a^{10}$ ) of -8.6 kcal/mol. This difference is consistent with Figure 2, which shows that in the ground vibrational state, the complex can sample the proton-shared region of the surface, thereby lowering the anharmonic  $\nu = 0$  level relative to the harmonic.

The equilibrium structure of BrH:NH<sub>3</sub> has a computed Br-N distance ( $R_e$ ) of 3.247 Å and a Br-H distance of 1.462 Å, which is slightly elongated relative to the monomer distance of 1.407 Å.<sup>9</sup> This structure is consistent with the description given by

(35) Barnes, A. J.; Wright, M. P. J. *Chem. Soc., Faraday Trans. 2* **1986**, 82, 153.

**Table 5.** Harmonic and Anharmonic Proton and Dimer Stretching Frequencies ( $\text{cm}^{-1}$ ) as a Function of Field Strength ( $\text{au}$ )<sup>a</sup>

field	harmonic				anharmonic			
	full surface		"triatomic" surface		dimer		proton	
	dimer	proton	dimer	proton	1-D	2-D	1-D	2-D
CIH:NH <sub>3</sub>								
0.0000	191	2289	189	2278	193	202	1905	1567
0.0010			185	2191	193	213	1740	1415
0.0025			220	2054	198	244	1388	1219
0.0040			220	1787	208	301	972	1067
0.0055			442	512	304	372	1072	936
0.0100			333	1812	327	383	1130	1137
0.0150			256	2437	246	274	1811	1781
expt (in Ar) <sup>35</sup>								1371
expt (in N <sub>2</sub> ) <sup>35</sup>								720
BrH:NH <sub>3</sub>								
0.0000	135	2006	133	1990	139	210	1469	908
0.0005			112	1883	141	252	1238	865
0.0010			376	1002	370	293	979	833
0.0025			351	1369	348	362	971	809
0.0040			342	1683	329	362	1054	954
0.0080			286	2180	277	305	1513	1544
0.0120			221	2259	214	240	2062	2041
expt (in Ar) <sup>35</sup>								729
expt (in N <sub>2</sub> ) <sup>35</sup>								1386
CIH:N(CH <sub>3</sub> ) <sub>3</sub>								
0.0000	485	b	314	1406	310	320	1344	1134
0.0010			303	1579	298	316	1370	1221
0.0040			272	1938	266	289	1499	1478
expt (in Ar) <sup>35</sup>								1486
expt (in N <sub>2</sub> ) <sup>35</sup>								1615
BrH:N(CH <sub>3</sub> ) <sub>3</sub>								
0.0000	199	2095	232	2004	230	239	1622	1595
0.0010			226	2102	224	233	1697	1683
0.0040			209	2326	205	214	1926	1933
expt (in Ar) <sup>35</sup>								1660
expt (in N <sub>2</sub> ) <sup>35</sup>								1890
								1872

<sup>a</sup> Based on MP2/aug'-cc-pVDZ data for HCl complexes and MP2/6-31+G(d,p) data for HBr complexes. <sup>b</sup> There are three strong bands with proton-stretching character at 1588, 1383, and 1185  $\text{cm}^{-1}$ . See text.

Legon that proton transfer from Br to N does not occur in this complex.<sup>34</sup> However, the potential surface surrounding the global minimum is relatively flat, and a Born-Oppenheimer minimum with a proton-shared hydrogen bond lies relatively close in energy to the global minimum. The ground-state vibrational wave function is centered in a shallow valley which connects the two minima, and both the traditional and the proton-shared regions of the potential surface are accessible in the ground ( $\nu = 0$ ) and first excited ( $\nu = 1$ ) states of the proton-stretching mode, as evident from Figures 2 and 3. A very large anharmonicity correction may be anticipated for the proton-stretching vibration in this complex. [The existence of a second minimum on this surface should not be overemphasized. The MP2/6-31+G(d,p) barrier separating these two minima is less than 0.01 kcal/mol as measured from the higher-energy structure. Moreover, this second minimum is not found on the MP2/aug'-cc-pVDZ surface. The anharmonic treatment vibrational averages over such low-energy features so these do not influence the computed anharmonic frequencies.]

Harmonic and anharmonic frequencies for BrH:NH<sub>3</sub> are reported in Table 5. The pseudo-triatomic and full dimensional harmonic proton-stretching frequencies are 1990 and 2006  $\text{cm}^{-1}$ , respectively. A one-dimensional anharmonic treatment of the proton-stretching vibration along the normal coordinate for the proton stretch on the two-dimensional surface gives a frequency

of 1469  $\text{cm}^{-1}$ . The two-dimensional anharmonic frequency is further reduced to 908  $\text{cm}^{-1}$ , but still remains higher than the Ar matrix value of 729  $\text{cm}^{-1}$ .<sup>35</sup> However, the computed two-dimensional proton-stretching frequency is lower than the experimental frequency measured in an N<sub>2</sub> matrix, which is 1386  $\text{cm}^{-1}$ .<sup>35</sup> We will demonstrate below that computed two-dimensional anharmonic proton stretching frequencies for both CIH:NH<sub>3</sub> and BrH:NH<sub>3</sub> obtained from surfaces generated in the presence of external electric fields can resolve these discrepancies and provide insight into the effects of the matrix on the vibrational spectra of these complexes.

(c) CIH:N(CH<sub>3</sub>)<sub>3</sub>. As noted in a previous study, the degree of proton transfer from hydrogen halides to a series of related bases increases as the proton affinity of the base increases.<sup>11,12</sup> The proton affinity of trimethylamine (225.1 kcal/mol)<sup>36</sup> is greater than that of ammonia (204.0 kcal/mol),<sup>36</sup> so that both the stabilities and the degree of proton transfer should be greater in complexes with N(CH<sub>3</sub>)<sub>3</sub> than in the corresponding complexes with NH<sub>3</sub>. The MP2/aug'-cc-pVDZ binding energy of CIH:N(CH<sub>3</sub>)<sub>3</sub> is -17.8 kcal/mol, while the binding enthalpies ( $\Delta H_{\text{h}}^{10}$  and  $\Delta H_{\text{a}}^{10}$ ) are -14.6 and -15.2 kcal/mol, respectively. The relatively large error in the zero-point contribution obtained from the harmonic frequencies is a consequence of the inability of the harmonic approximation to describe the region surrounding the global minimum, which is relatively broad and flat, as indicated in Figure 2. These binding energies and enthalpies are significantly larger than the corresponding energy and enthalpies of CIH:NH<sub>3</sub>, as evident from Table 4.

The equilibrium structure of CIH:N(CH<sub>3</sub>)<sub>3</sub> is stabilized by a proton-shared hydrogen bond, as seen from the structural data of Table 3. The computed Cl-N and Cl-H distances ( $R_{\text{e}}$ ) are 2.825 and 1.658 Å, respectively, significantly longer than the corresponding distances in CIH:NH<sub>3</sub>, and typical for complexes with proton-shared Cl...H...N hydrogen bonds.<sup>11,12</sup> Legon measured a Cl-N distance ( $R_0$ ) of 2.816 Å, and concluded from his microwave experiments that there is an appreciable extent of proton transfer from Cl to N in this complex.<sup>34</sup> It should be noted, however, that the proton is not fully transferred to N. The CIH:N(CH<sub>3</sub>)<sub>3</sub> complex has neither the structural (short N-H bond length) nor the vibrational spectroscopic properties (high-frequency N-H stretching band) associated with a hydrogen-bonded N-H<sup>+</sup>...Cl<sup>-</sup> ion pair.<sup>11,12</sup>

The computed MP2/aug'-cc-pVDZ harmonic spectrum of CIH:N(CH<sub>3</sub>)<sub>3</sub> is typical of spectra arising from complexes with proton-shared hydrogen bonds, exhibiting several strong, low-frequency bands.<sup>11,12,37,38</sup> There is a strong proton-stretching band at 1588  $\text{cm}^{-1}$  and two weaker bands of approximately equal intensities at 1383 and 1184  $\text{cm}^{-1}$ . The normal coordinate displacement vectors for these bands indicate that all three involve the hydrogen-bonded proton stretch coupled to CH<sub>3</sub> vibrational modes. The band at 1383  $\text{cm}^{-1}$  couples the proton stretch to CH<sub>3</sub> inversion. The strongest band in the experimental Ar matrix spectrum of CIH:N(CH<sub>3</sub>)<sub>3</sub> is found at 1486  $\text{cm}^{-1}$ , and has been assigned to the proton-stretching vibration by Barnes.<sup>35</sup> The frequency of this band increases to 1615  $\text{cm}^{-1}$  in an N<sub>2</sub> matrix.<sup>35</sup> It should be noted that for CIH:NH<sub>3</sub> the proton-stretching frequency is significantly lower in N<sub>2</sub> than in Ar, but for the complex CIH:N(CH<sub>3</sub>)<sub>3</sub> the reverse is true. For this complex, the harmonic proton stretching frequency is

(36) Lias, S. G.; Bartmess, J. E.; Liebman, J. F.; Holmes, J. L.; Levin, R. D.; Mallard, W. G. *J. Phys. Chem. Ref. Data* **1988**, Suppl. 1.

(37) Del Bene, J. E.; Szczepaniak, K.; Chabrier, P.; Person, W. B. *J. Phys. Chem. A* **1997**, *101*, 4481.

(38) Szczepaniak, K.; Chabrier, P.; Person, W. B.; Del Bene, J. E. *J. Mol. Struct.* **1997**, *436-437*, 367.



fortuitously close to the experimental frequencies measured in both Ar and N<sub>2</sub>.

A one-dimensional anharmonic treatment of the proton-stretching vibration along the normal coordinate vector from the pseudo-triatomic two-dimensional surface yields a vibrational frequency of 1344 cm<sup>-1</sup>. Direct comparison with harmonic frequencies from the full surface is not possible, since in the two-dimensional treatment the geometry of N(CH<sub>3</sub>)<sub>3</sub> is frozen. Treating the coupling of the hydrogen-bonded stretch to intramolecular motions is a subject for future study using higher dimensional surfaces. Nevertheless, the two-dimensional anharmonic proton-stretching frequency is 1134 cm<sup>-1</sup>, which is lower than the experimental frequencies measured by Barnes in Ar and N<sub>2</sub> matrices. We suggest that the computed two-dimensional anharmonic frequency would correspond to an experimental frequency if such were measured in the gas phase. The effects of Ar and N<sub>2</sub> matrices will be addressed below.

In complexes with proton-shared hydrogen bonds, the proton stretching vibration may be characterized either as a perturbed Cl-H stretch or a perturbed N-H stretch, depending on the magnitude of the Cl-H and N-H stretching force constants. In a previous study,<sup>39</sup> the quasisymmetric hydrogen bond was defined as a proton-shared hydrogen bond in which Cl-H and N-H stretching force constants are equal, and the proton-stretching frequency is at a minimum along a curve relating the proton-stretching frequency to the Cl-H distance. The region of the proton-shared hydrogen bond extends on both sides of the quasisymmetric hydrogen bond, on one side being better described as a perturbed Cl-H stretching vibration and on the other as a perturbed N-H stretching vibration. In ClH:N(CH<sub>3</sub>)<sub>3</sub> the proton-stretching band is dominated by N-H stretching character. This is evident from Figures 2 and 3, which show the square of the vibrational wave functions for the ground and the  $\nu = 1$  states of the proton-stretching vibration, respectively, superimposed on the potential surfaces. The minimum on the ClH:N(CH<sub>3</sub>)<sub>3</sub> surface is found in the proton-shared region, and the ground-state wave function is centered near the minimum. The wave function for the  $\nu = 1$  state of the proton-stretching mode indicates that in this state, the complex accesses that region of the potential surface associated with a traditional Cl-H...N hydrogen bond.

The full (complete dimensional) surface harmonic dimer stretching frequency for ClH:N(CH<sub>3</sub>)<sub>3</sub> is quite high at 485 cm<sup>-1</sup>, which suggests that the harmonic approximation is describing what could be viewed as a low-frequency Cl-H stretch in a complex with long Cl-H and N-H bonds. On the pseudotriatomic surface, the harmonic frequency has a value of 314 cm<sup>-1</sup>. The one- and two-dimensional anharmonic frequencies for the dimer stretch are essentially identical at 310 and 320 cm<sup>-1</sup>. This vibration has not been observed experimentally.

**(d) BrH:N(CH<sub>3</sub>)<sub>3</sub>.** The complex BrH:N(CH<sub>3</sub>)<sub>3</sub> is the most stable of all complexes considered in this work, with computed MP2/6-31+G(d,p) binding energy and enthalpies ( $\Delta E_e$ ,  $\Delta H_h^{10}$ , and  $\Delta H_a^{10}$ ) of -26.7, -21.9, and -22.1 kcal/mol, respectively. These values are significantly greater than the corresponding binding energy and enthalpies of BrH:NH<sub>3</sub>, as seen in Table 4. The zero-point energy contributions obtained from the harmonic and anharmonic frequencies are very similar, since the anharmonicity of the potential surface is most evident in the  $\nu = 1$  state of the proton-stretching mode, as shown in Figures 2 and 3.

The equilibrium structure of BrH:N(CH<sub>3</sub>)<sub>3</sub> has computed Br-N and Br-H distances ( $R_e$ ) of 2.983 and 1.870 Å, respectively. A structure of this type was also reported by Latajka et al.<sup>40</sup> Comparison of the computed distances with corresponding distances in the complexes BrH:4-R-pyridine suggests that the equilibrium structure of BrH:N(CH<sub>3</sub>)<sub>3</sub> approaches that of a hydrogen-bonded ion pair.<sup>12</sup> This designation is also consistent with the computed harmonic spectrum of this complex, which exhibits a very strong proton-stretching band at 2095 cm<sup>-1</sup>, an N-H stretch perturbed by hydrogen bond formation. Legon reported an experimental Br-N distance of 2.96 Å and characterized this complex as one in which proton transfer from Br to N occurs.<sup>34</sup> The degree of proton transfer in this complex is greater than that found in ClH:N(CH<sub>3</sub>)<sub>3</sub>, a reflection of the greater proton-donating ability of HBr.

The square of the wave functions for the ground ( $\nu = 0$ ) and first excited ( $\nu = 1$ ) states of the proton-stretching vibration are shown superimposed on the two-dimensional BrH:N(CH<sub>3</sub>)<sub>3</sub> surface in Figures 2 and 3, respectively. These plots are consistent with the designation that the proton-stretching vibration in this complex is a perturbed N-H stretch. The ground state wave function is centered over the minimum on the potential surface, and shows predominately N-H stretching character. The plot for the  $\nu = 1$  state has appreciable probability in the region of the traditional hydrogen bond, indicating that this region is accessible in the first excited state of this vibration.

The computed full-dimensional harmonic spectrum of BrH:N(CH<sub>3</sub>)<sub>3</sub> exhibits a very strong band at 2095 cm<sup>-1</sup>, while the harmonic one-dimensional frequency obtained from the pseudotriatomic surface is 2004 cm<sup>-1</sup>. The computed one-dimensional anharmonic proton-stretching frequency is 1622 cm<sup>-1</sup>, while the two-dimensional frequency is only slightly lower at 1595 cm<sup>-1</sup>. This suggests that coupling between the proton- and dimer-stretching modes is not as important in this complex as in the other three complexes discussed above. The experimental proton-stretching bands in Ar and N<sub>2</sub> matrices have been assigned to absorptions at 1660 cm<sup>-1</sup> in Ar, and a doublet at 1890 and 1872 cm<sup>-1</sup> in N<sub>2</sub>.<sup>35</sup>

**Structural and Spectral Data for Complexes in External Fields of Varying Strengths.** When an external electric field is applied along the X-H-N direction in these complexes, the field preferentially stabilizes geometries in which there is charge separation along the X-N axis. Since complexes with proton-shared hydrogen bonds have larger dipole moments, external fields stabilize this type of structure relative to a traditional hydrogen-bonded structure, with the amount of stabilization increasing with increasing field strength. If the field is strong enough, full proton transfer occurs, resulting in a hydrogen-bonded ion pair N-H<sup>+</sup>...X<sup>-</sup>. Such external fields, whether induced as a result of a relatively weak interaction with a polarizable matrix material or with a solvent of high dielectric constant, will influence the structure of the complex and the nature and frequency of the dimer and proton-stretching vibrations.

Appropriate field strengths for complexes within an Ar matrix may be calculated using Onsager's equation for the reaction field,  $\mathbf{R}$ , at a point dipole in a cavity within a continuous dielectric medium.<sup>14</sup> In atomic units

$$\mathbf{R} = [2(\epsilon - 1)/(2\epsilon + 1)]\mathbf{m}/a^3 \quad (1)$$

where  $\epsilon$  is the relative permittivity of the dielectric medium (solid argon, for example),  $\mathbf{m}$  is the total dipole moment of the complex, and  $a$  is the cavity radius. The total dipole moment may be written as

(39) Szczepaniak, K.; Chabrier, P.; Person, W. B.; Del Bene, J. E. *J. Mol. Struct.* In press.

(40) Latajka, Z.; Scheiner, S.; Ratajczak, H. *Chem. Phys.* **1992**, *166*, 85.

$$\mathbf{m} = \mu + \alpha \mathbf{R} \quad (2)$$

where  $\mu$  is the permanent dipole moment and  $\alpha$  is the (isotropic) polarizability of the complex. The correction due to the reaction field is likely to be small and we approximate  $\mathbf{m} = \mu$ . The cavity radius may be calculated by determining the volume contained within the 0.001 au electron density surface around the complex. The radius,  $r$ , of a sphere with this volume can be calculated<sup>33</sup> and the cavity radius,  $a$ , is given by  $r + 0.5 \text{ \AA}$ .

Sample calculations were performed at MP2/aug'-cc-pVDZ and MP2/6-31+G(d,p) for ClH:NH<sub>3</sub> and BrH:NH<sub>3</sub>, respectively. Cavity radii and dipole moments for these complexes are given in Table 6. In earlier work<sup>9,10</sup> we considered three argon atoms explicitly arranged around complexes of FH:NH<sub>3</sub>, ClH:NH<sub>3</sub>, and BrH:NH<sub>3</sub>. The MP2/6-31+G(d,p) optimized distance of each argon atom from the Cl-N axis in ClH:NH<sub>3</sub> was 6.67 bohr. In BrH:NH<sub>3</sub>, this distance was 6.70 bohr. These values are similar to the cavity radii calculated in the present work. In paper 10, the computed stabilization energy of the BrH:NH<sub>3</sub> complex by three argon atoms was compared with classical electrostatic charge/induced-dipole and dipole/induced-quadrupole interactions. In the present work we focus on the bulk effects of a matrix on the various hydrogen-bonded complexes. The Onsager reaction field model is expected to provide a more realistic description of these effects than calculations involving small clusters.

Solid Ar has a relative permittivity  $\epsilon = 1.61$ <sup>41</sup> and, at approximately 10 K, solid N<sub>2</sub> has a relative permittivity at audio frequencies of 1.43.<sup>42</sup> The relative permittivity of solid N<sub>2</sub>, however, is sensitive to the preparation of the sample; the N<sub>2</sub> matrix is typically annealed in IR experiments and this will raise its relative permittivity.<sup>42</sup> However, it is known that, relative to the gas phase, N<sub>2</sub> matrices have a larger effect on IR spectra than Ar matrices,<sup>43</sup> suggesting an effective relative permittivity greater than 1.6. For illustrative purposes the Onsager reaction field has been calculated at values of  $\epsilon = 1.6$  and 2.0, and the results are shown in Table 6. It is apparent from Table 6 that, although there is a large change in dipole between the traditional and proton-shared structures for BrH:NH<sub>3</sub>, the cavity radius also changes and there is a relatively small variation in the reaction field. The approximation of an isotropic field to model the inert matrix is therefore not as extreme as may have been expected.

The potential energy surfaces generated in this study have been calculated at field strengths of 0.0010, 0.0025, 0.0040, 0.0055, 0.0100, and 0.0150 au for ClH:NH<sub>3</sub> and at field strengths of 0.0005, 0.0010, 0.0025, 0.0040, 0.0080, and 0.0120 au for BrH:NH<sub>3</sub>. The highest field strengths have been used for illustrative purposes. Field strengths of 0.0010 and 0.0040 au have been used to calculate potential energy surfaces for ClH:N(CH<sub>3</sub>)<sub>3</sub> and BrH:N(CH<sub>3</sub>)<sub>3</sub>. Comparison with experiment indicates that the effects of Ar and N<sub>2</sub> matrices are consistent with the application of reaction fields of the order of those in Table 6.

**(a) ClH:NH<sub>3</sub>.** As noted above, the potential energy surface for ClH:NH<sub>3</sub> at zero field has a minimum located in that region of the surface associated with a traditional Cl-H...N hydrogen bond. As external electric fields of increasing strengths are applied, the minimum moves along the surface in a valley connecting the traditional and proton-shared regions, and acquires increased proton-shared character. This is illustrated in Figure 4 which shows the square of the ground-state

**Table 6.** The Dipole Moment, Cavity Radius, and Onsager Reaction Field for the Equilibrium Geometry of ClH:NH<sub>3</sub> and the Traditional (T) and Proton-Shared (PS) Structures of BrH:NH<sub>3</sub> at  $\epsilon = 1.6$  and 2.0

species	dipole moment (D)	cavity radius, $a$ (bohr)	reaction field, $R$ (au)	
			$\epsilon = 1.6$	$\epsilon = 2.0$
ClH:NH <sub>3</sub>	5.85	6.55	0.0019	0.0027
BrH:NH <sub>3</sub> (T)	4.79	6.98	0.0022	0.0031
BrH:NH <sub>3</sub> (PS)	8.40	6.24	0.0029	0.0040

vibrational wave functions superimposed on the potential surfaces at fields of 0.0010, 0.0025, 0.0040, 0.0055, 0.0100, and 0.0150 au, respectively. At the lower field strengths of 0.0010, 0.0025, and 0.0040 au, the minimum progressively moves away from the region of the traditional Cl-H...N hydrogen bond toward the proton-shared Cl...H...N region of the surface. At a field of 0.0055 au, the minimum in the potential surface is very broad, encompassing both the traditional and proton-shared regions. The wave function is essentially centered in this very broad valley. As the field increases to 0.0100 au, the minimum still corresponds to a proton-shared hydrogen bond, but now the wave function exhibits greater N-H...Cl character. Further increasing the field leads to a more sharply defined minimum and a wave function that describes a hydrogen-bonded ion pair.

The equilibrium Cl-N and Cl-H distances [ $R_e(\text{Cl-N})$  and  $R_e(\text{Cl-H})$ ] determined from the potential surfaces and the expectation values of the Cl-N and Cl-H distances [ $R_0(\text{Cl-N})$  and  $R_0(\text{Cl-H})$ ] computed from the ground-state vibrational wave functions at various field strengths are reported in Table 3. As the field strength increases, the Cl-H distance increases. In contrast, the Cl-N distance initially decreases with increasing field strength to a minimum distance at a field of 0.0055 au. The structure of the complex at this field strength has a proton-shared hydrogen bond that appears to be quite close to quasisymmetric, implying that the proton is equally shared between the Cl and N atoms, that is, the forces exerted by Cl and N on H are essentially equal. Further increasing the field strength results in an increasing Cl-N distance in structures that approach hydrogen-bonded ion pairs.

The computed anharmonic vibrational frequencies for the proton stretching mode are consistent with the graphical pictures of field effects. As the structure of the ClH:NH<sub>3</sub> complex moves further away from a traditional Cl-H...N hydrogen bond toward a proton-shared Cl...H...N hydrogen bond, the frequency of the proton-stretching vibration decreases, as is evident from Table 5. At a field strength of 0.0055 au, the anharmonic two-dimensional proton-stretching frequency has its lowest value of 936 cm<sup>-1</sup> in a complex in which the hydrogen bond is close to quasisymmetric. Increasing the field to 0.0100 au increases the anharmonic two-dimensional proton-stretching frequency to 1137 cm<sup>-1</sup>. At this field strength the proton is more closely associated with N than Cl, and the proton-stretching mode is better described as a perturbed N-H stretch. As the field increases further and the structure approaches a hydrogen-bonded ion pair, the N-H proton-stretching frequency increases to 1781 cm<sup>-1</sup>.

The differences between the harmonic frequencies and the one- and two-dimensional anharmonic frequencies for ClH:NH<sub>3</sub> are most interesting. The harmonic proton-stretching frequencies are always too high relative to the anharmonic frequencies except at a field strength of 0.0055 au, where the hydrogen bond is essentially quasisymmetric. Because both the Cl-H and N-H bonds are long and relatively weak in this structure, both the "dimer" and the "proton" stretches are predicted to be very low

(41) Marcoux, J. J. *Opt. Soc. Am.* **1969**, *59*, 998.

(42) Pilla, S.; Hamida, J. A.; Muttalib, K. A.; Sullivan, N. S. *Phys. Lett. A* **1999**, *256*, 75.

(43) Jacox, M. E. *J. Phys. Chem. Ref. Data* **1994**, Monograph No. 3.



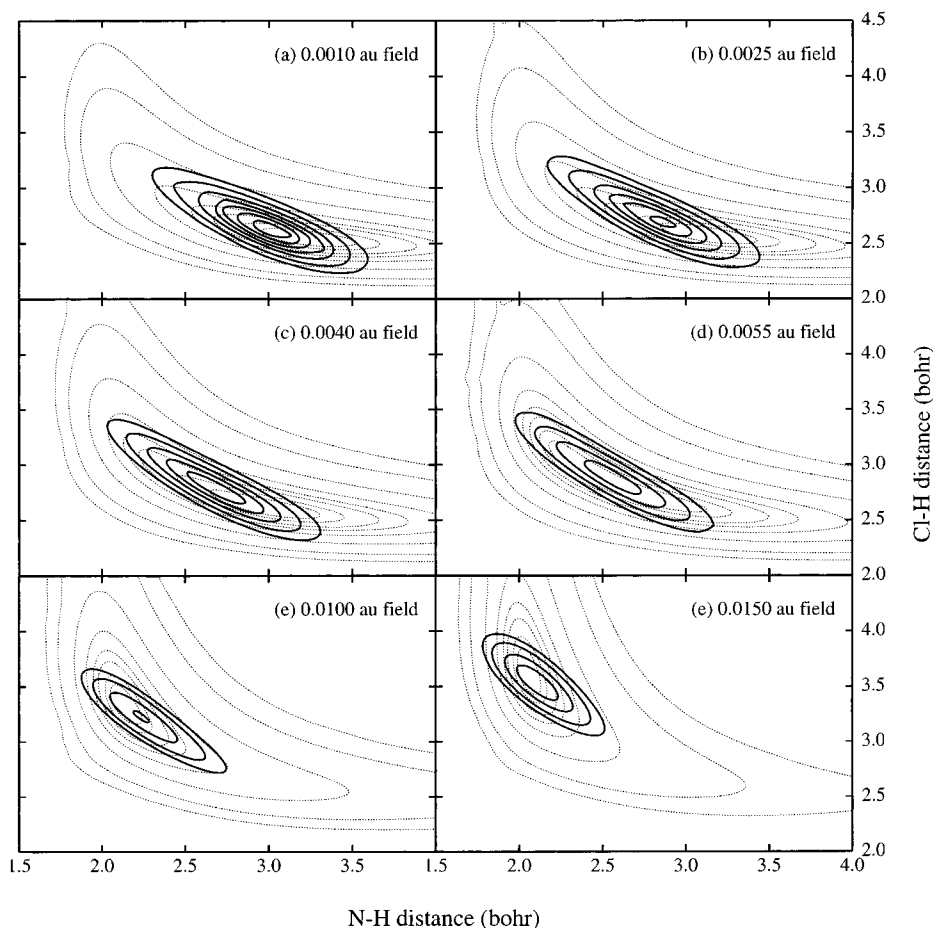


**Figure 4.** Square of the ground-state vibrational wave functions for ClH:NH<sub>3</sub> superimposed on the potential surfaces at field strengths of (from left to right) 0.0010, 0.0025, 0.0040, 0.0055, 0.0100, and 0.0150 au.

at 442 and 512  $\text{cm}^{-1}$  in the harmonic approximation. In this simple picture, if the proton stretch is viewed as a very perturbed Cl–H stretch, then the dimer stretch might also be viewed as a perturbed N–H stretch. In contrast, the one- and two-dimensional anharmonic frequencies maintain a distinction between the proton and dimer stretches at all field strengths. The one-dimensional proton-stretching frequency exhibits a minimum at a lower field strength of 0.0040 au, and for this field, the two-dimensional frequency is higher than the one-dimensional frequency. This again emphasizes the importance of a two-dimensional treatment for this complex. At the higher fields of 0.0100 and 0.0150 au, however, the difference between the one- and two-dimensional anharmonic proton-stretching frequencies decreases, suggesting that the degree of coupling between proton and heavy-atom motion is reduced as the heavy atom distance increases.

It was noted above that the zero-field anharmonic two-dimensional proton-stretching frequency of 1567  $\text{cm}^{-1}$  is about 200  $\text{cm}^{-1}$  higher than the experimental Ar matrix frequency of 1371  $\text{cm}^{-1}$ .<sup>35</sup> The data of Table 5 indicate that a weak field between 0.0010 and 0.0025 au would be sufficient to reduce the computed two-dimensional proton-stretching frequency and bring it into better agreement with the Ar matrix frequency, and indeed, these fields are what may be expected in an Ar matrix. A field between 0.0040 and 0.0100 would further reduce the computed two-dimensional proton-stretching frequency, and bring it into better agreement with the experimental frequency obtained in an N<sub>2</sub> matrix. However, it should be noted that the anharmonic treatment of vibration reported here is based upon a two-dimensional surface which neglects other vibrational

motions of the complex (e.g., the NH<sub>3</sub> inversion mode) which might couple to the proton-stretching motion. Future studies will address the anharmonicity of the proton-stretching motion in higher dimensions, and the assignment of the entire ClH:NH<sub>3</sub> spectrum.

Figure 3 shows a plot of the square of the wave function for the  $\nu = 1$  state of the proton-stretching vibration in ClH:NH<sub>3</sub> at zero field. This plot indicates graphically the extent to which the proton-shared region of the surface can be accessed in this state, and why an anharmonic treatment is necessary for the proton-stretching mode. Similar plots have been obtained for the  $\nu = 1$  state of the proton-stretching mode at different field strengths. At fields of 0.0000, 0.0025, and 0.0100 au, the wave functions are easily interpretable. At a field of 0.0025 au the proton stretch is predominately a perturbed Cl–H stretch which samples the proton-shared region of the surface, similar to the situation at zero field. At a field of 0.0100 au, the proton stretch is a perturbed N–H stretch, and the plot for the  $\nu = 1$  state indicates that it is the region of the surface associated with the traditional hydrogen bond that is accessible in the  $\nu = 1$  state of the proton-stretching vibration. For the remaining fields, the plots do not exhibit systematic patterns due to considerable mixing of overtone bands for the dimer stretch with the fundamental proton stretch, which leads to more complicated nodal patterns. This mixing arises from accidental near degeneracies between the proton stretching frequency and the frequency of an overtone of the dimer stretch. The nature of the mixing of the proton and dimer wave functions is summarized in Table 7.

**Table 7.** Accidental Degeneracies Involving the Fundamental Proton-Stretching Frequency ( $\text{cm}^{-1}$ ) and Overtones of the Dimer-Stretching Vibration in  $\text{ClH:NH}_3$  and  $\text{BrH:NH}_3$  at Various Fields (au)<sup>a</sup>

field	designation	proton-stretch freq	designation	dimer overtone
		$\text{ClH:NH}_3$		
0.0010	(0,1)	1415	(7,0)	1429
0.0040	(0,1)	1067	(3,0)	1035
0.0055	(0,1)	936	(3,0)	967
		$\text{BrH:NH}_3$		
0.0010	(0,1)	833	(4,0)	865
0.0025	(0,1)	809	(3,0)	935

<sup>a</sup> (x,y): x refers to the dimer stretch, and y to the proton stretch; (0,1) is the fundamental for the proton stretch; (n,0) is the (n - 1)th overtone of the dimer stretch.

**(b)  $\text{BrH:NH}_3$ .** As noted above, the potential energy surface at zero field for  $\text{BrH:NH}_3$  has a minimum associated with a traditional  $\text{Br-H}\cdots\text{N}$  hydrogen bond, with a valley which extends to the region of the proton-shared hydrogen bond. At a field of 0.0005 au, the minimum moves further along the valley toward the proton-shared region. At a field of 0.0010 au, there is a double minimum in the potential surface, one associated with a traditional hydrogen-bonded structure, and the second with a proton-shared structure. As the field increases a single minimum reappears, this time located in the proton-shared region of the surface, and a valley extends from this minimum toward the region of the traditional hydrogen bond. As the field increases further to 0.0040, 0.0080, and 0.0120 au, the single minimum moves further away from the region of the traditional hydrogen-bonded complex, and at higher fields becomes deeper and better defined.

The square of the wave functions for the ground vibrational state of  $\text{BrH:NH}_3$  at the various field strengths is shown superimposed on the corresponding potential surfaces in Figure 5. The plots for fields of 0.0005 and 0.0010 au are very similar to the plots for zero field, with the wave functions positioned in the valley that connects the traditional and proton-shared regions of the surface. As the field increases to 0.0025 au, the wave function moves further toward the proton-shared region, but is displaced from the minimum toward the region of the traditional hydrogen bond. At higher fields of 0.0040, 0.0080, and 0.0120 au the wave function becomes more highly localized, until at the highest field, the wave function looks very much like that anticipated for a hydrogen-bonded  $\text{N-H}^+\cdots\text{Br}^-$  ion pair.

As noted above, at zero field there is a significant difference between the computed harmonic proton-stretching vibrational frequencies and the anharmonic one- and two-dimensional frequencies. This difference remains as the field strength increases, with the harmonic frequency obtained from the pseudotriatomic surface always significantly overestimating the anharmonic frequencies, as seen in Table 5. In contrast, while the one-dimensional anharmonic frequency for the proton-stretching vibration does decrease, there is little change in the computed two-dimensional anharmonic proton-stretching frequencies which decrease by about  $100\text{ cm}^{-1}$  as the external field strength increases from 0.0005 to 0.0025 au. It is important to note that although there are two minima on the surface that are separated by a small barrier at a field strength of 0.0010 au, the existence of a double minimum is inconsequential in view of vibrational averaging in a two-dimensional anharmonic treatment.

The two-dimensional proton-stretching frequency attains its minimum value of  $809\text{ cm}^{-1}$  at a field strength of 0.0025 au, a

value that is only  $80\text{ cm}^{-1}$  higher than the experimental Ar matrix value. This hydrogen-bonded complex most closely corresponds to a quasi-symmetric hydrogen-bonded complex, with the proton approximately equally shared between Br and N. As the field strength increases, the proton stretching frequency increases, and assumes greater N-H character. As the field increases from 0.0025 to 0.0040 to 0.0080 au, the proton-stretching frequency increases from 809 to 954 to  $1544\text{ cm}^{-1}$ , respectively. The experimental proton-stretching frequency of  $\text{BrH:NH}_3$  in  $\text{N}_2$  is  $1386\text{ cm}^{-1}$ , a value that corresponds to a field strength between 0.0040 and 0.0080 au. At the highest field of 0.0120 au, the proton stretch is best described as a perturbed N-H stretch in a hydrogen-bonded ion pair, with a two-dimensional N-H proton-stretching frequency of  $2041\text{ cm}^{-1}$ .

The wave functions for the  $\nu = 1$  state of the proton stretching mode are not shown, but they are consistent with the interpretations presented above. In contrast to  $\text{ClH:NH}_3$ , there is a relatively small amount of mixing of overtones of the dimer stretch with the fundamental for the proton stretch. Some mixing does occur at field strengths of 0.0010 and 0.0025 au, and the nature of this mixing is summarized in Table 7.

**(c)  $\text{ClH:N(CH}_3)_3$ .** The MP2/aug'-cc-pVDZ equilibrium structure of  $\text{ClH:N(CH}_3)_3$  at zero field has a proton-shared  $\text{Cl}\cdots\text{H}\cdots\text{N}$  hydrogen bond, and the potential surface exhibits a single minimum in the proton-shared region. As external fields of increasing strength are applied, the minimum moves toward shorter N-H (and therefore longer Cl-H) distances, as expected. The square of the ground state wave functions superimposed on the surfaces for field strengths of 0.0000, 0.0010, and 0.0040 au is shown in Figure 6. These functions tend to be located over the minimum on the surface, although they are slightly displaced toward the region of the traditional  $\text{Cl-H}\cdots\text{N}$  hydrogen bond. As the field strength increases, the wave functions move further from the proton-shared region and become more localized. It is anticipated that at slightly higher fields, the wave functions would be those corresponding to a hydrogen-bonded  $\text{N-H}^+\cdots\text{Cl}^-$  ion pair.

The square of the wave functions for the  $\nu = 1$  state of the proton-stretching mode is also shown in Figure 6. These show that in this excited vibrational state, the system does sample the region of the surface associated with a traditional  $\text{Cl-H}\cdots\text{N}$  hydrogen bond. For this system, there is no mixing of overtones of the dimer stretch with the fundamental proton stretch.

The pseudotriatomic harmonic frequencies for the dimer stretch obtained at fields of 0.0000, 0.0010, and 0.0040 au are in agreement with the one- and two-dimensional anharmonic frequencies, but the harmonic frequency obtained from the full dimensional calculation at zero field is significantly higher. The harmonic frequencies for the proton stretch are also too high, a result of the anharmonicity of the surface. As the field increases, both the one- and two-dimensional anharmonic frequencies increase, but the difference between them decreases with increasing field strength. This again suggests that coupling between proton and dimer motions is less important as the complex approaches a hydrogen-bonded ion pair and the Cl-N distance increases.

In contrast to  $\text{ClH:NH}_3$  and  $\text{BrH:NH}_3$ , imposing even a small external electric field leads to an increase in the proton-stretching frequency of  $\text{ClH:N(CH}_3)_3$ . This suggests that at zero field, this complex lies either at, or on the ion-pair side of, the idealized quasisymmetric hydrogen-bonded complex. Examination of the potential surface along the proton-stretching normal mode

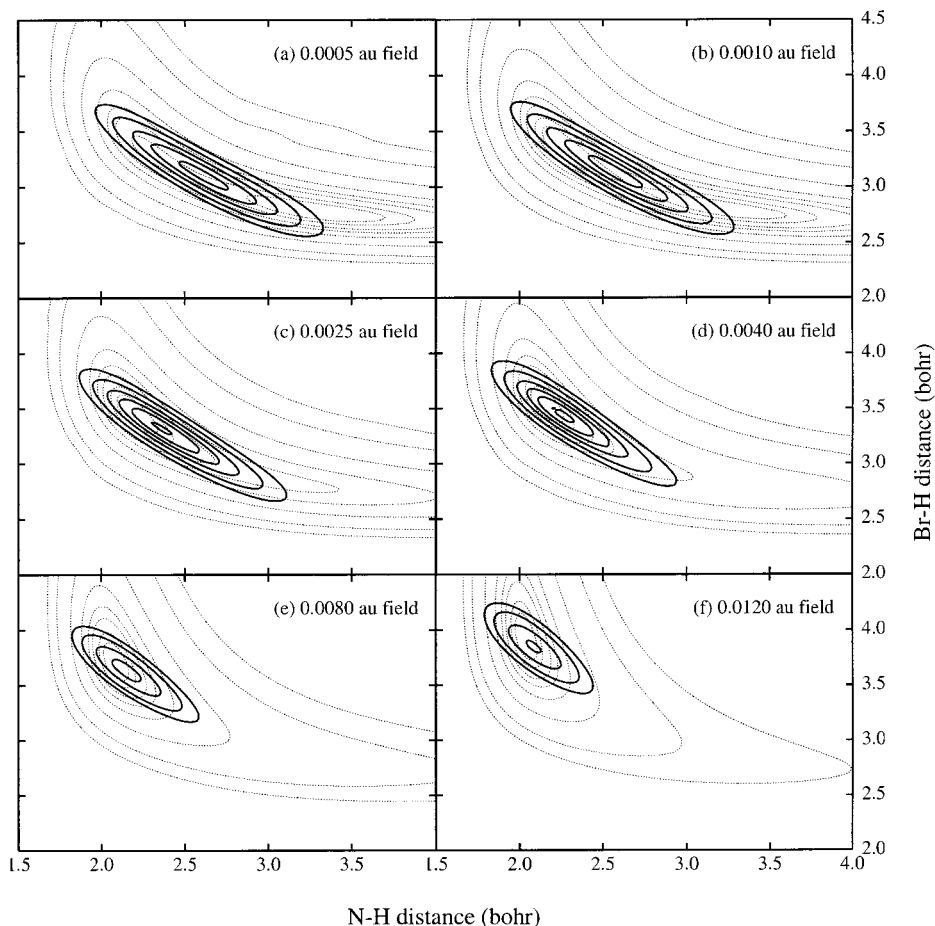


**Figure 5.** Square of the ground-state vibrational wave functions for BrH:NH<sub>3</sub> superimposed on the potential surfaces at field strengths of (from left to right) 0.0005, 0.0010, 0.0025, 0.0040, 0.0080, and 0.0120 au.

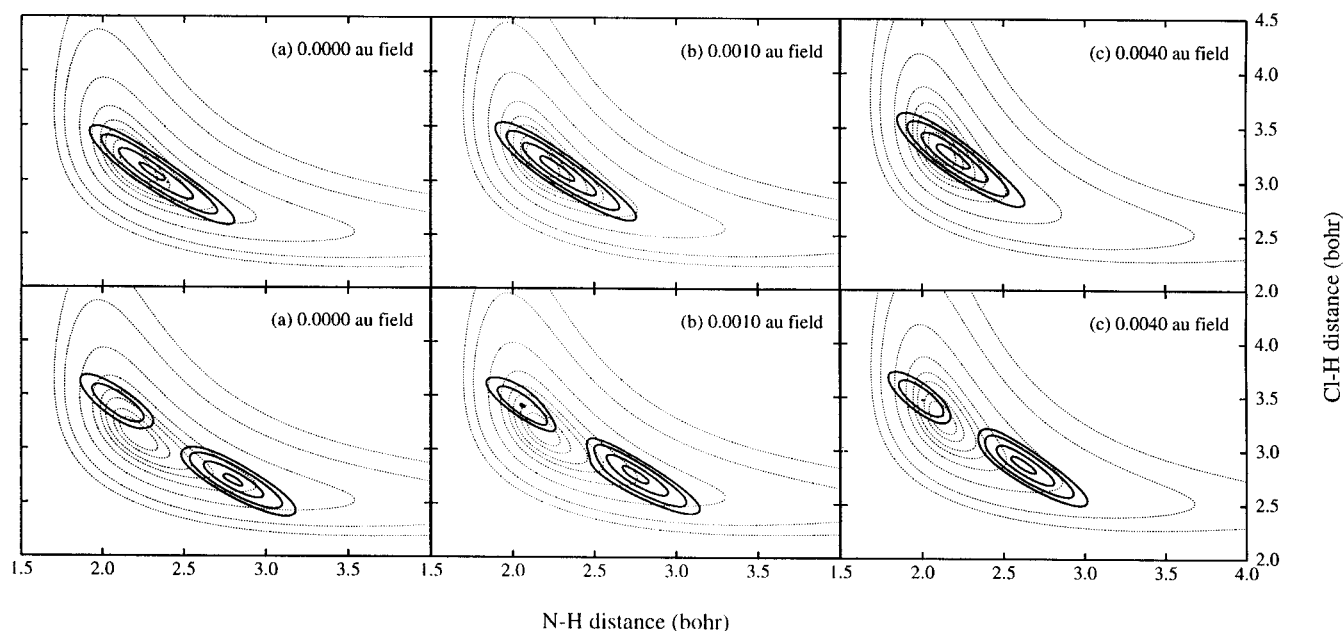


**Figure 6.** Square of the wave functions for the ground state (top) and  $\nu = 1$  state of the proton-stretching vibration (bottom) for ClH:N(CH<sub>3</sub>)<sub>3</sub> superimposed on the potential surface at fields of (a) 0.0000, (b) 0.0010, and (c) 0.0040 au.

confirms that the zero-field structure is just on the ion-pair side of quasisymmetric. Imposing an external field of any strength simply increases the ion-pair character. As a consequence, at a field of 0.0040 au, the computed anharmonic frequency for the proton-stretching vibration is 1478 cm<sup>-1</sup>, and in good agreement with the experimental Ar matrix frequency of 1486 cm<sup>-1</sup>.<sup>35</sup> It

is apparent that at a slightly higher field, the proton-stretching frequency would increase, and become comparable to the frequency of 1615 cm<sup>-1</sup> measured in an N<sub>2</sub> matrix.<sup>35</sup>

**(d) BrH:N(CH<sub>3</sub>)<sub>3</sub>.** As noted above, the equilibrium structure of BrH:N(CH<sub>3</sub>)<sub>3</sub> at zero field approaches that of a hydrogen-bonded ion pair. The surface shows a single minimum with the



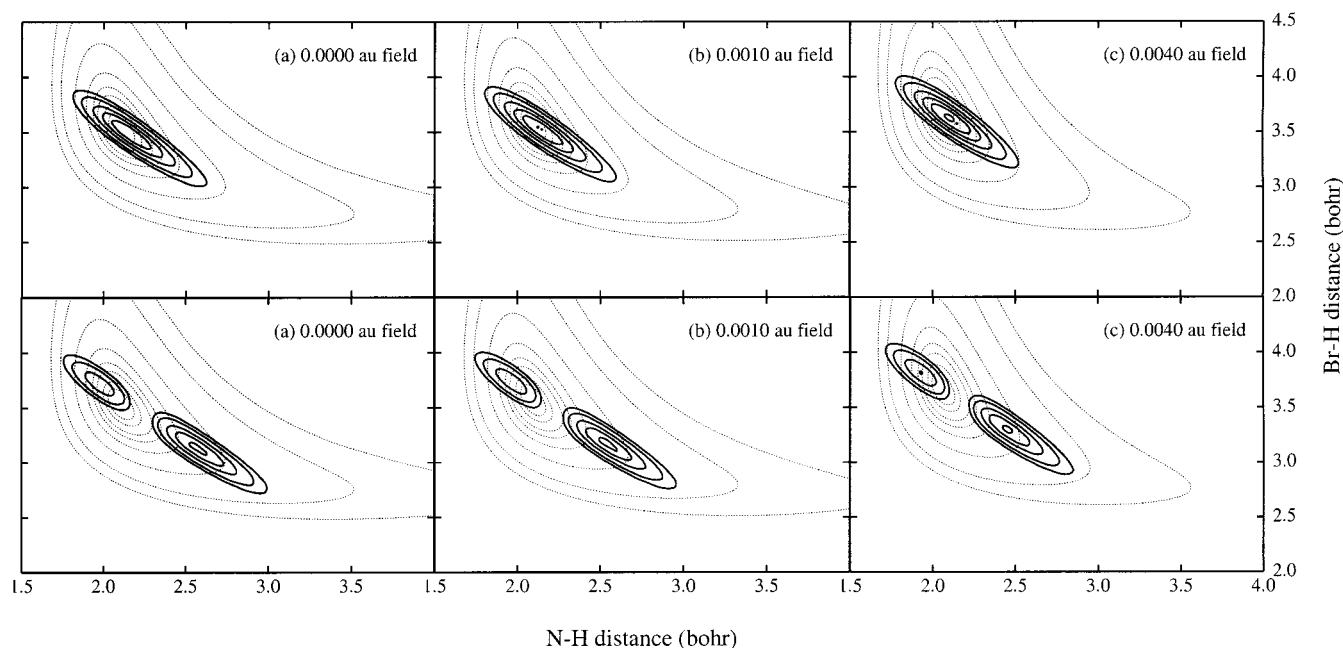


**Figure 7.** Square of the wave functions for the ground state (top) and  $\nu = 1$  state of the proton-stretching vibration (bottom) for  $\text{BrH:N}(\text{CH}_3)_3$  superimposed on the potential surface at fields of (a) 0.0000, (b) 0.0010, and (c) 0.0040 au.

minimum moving toward longer Br–H and Br–N distances with increasing field strength, as evident from Table 3. The square of the wave functions for the ground and the  $\nu = 1$  states of the proton-stretching vibrations is shown in Figure 7. The characteristics of these plots are quite similar to those for  $\text{ClH:N}(\text{CH}_3)_3$ , except that the degree of proton transfer at a given field is greater in  $\text{BrH:N}(\text{CH}_3)_3$ .

At zero field the harmonic frequency for the dimer stretch obtained from the full dimensional calculation of the vibrational spectrum is slightly lower than the pseudotriatomic harmonic frequency of  $232\text{ cm}^{-1}$ . The latter frequency is in good agreement with the corresponding anharmonic one- and two-dimensional frequencies, which also agree with each other, at all field strengths. The harmonic proton-stretching frequencies obtained from the full dimensional and the pseudotriatomic calculations are similar, but always too high. The one- and two-dimensional anharmonic frequencies for the proton-stretching vibration are similar, suggesting that there is little coupling between these motions. The two-dimensional proton stretching frequencies for  $\text{BrH:N}(\text{CH}_3)_3$  are also higher than those for  $\text{ClH:N}(\text{CH}_3)_3$  at equal field strengths, indicating that the ionic character of the  $\text{N-H}^+\cdots\text{X}^-$  hydrogen bond is greater in  $\text{BrH:N}(\text{CH}_3)_3$ .

The computed zero-field proton stretching frequency is  $1595\text{ cm}^{-1}$ , which is lower than the experimental values of  $1660$  and  $1890$  and  $1872\text{ cm}^{-1}$  in Ar and  $\text{N}_2$ , respectively.<sup>35</sup> Not surprisingly, applying an external electric field of  $0.0010$  au increases the proton-stretching frequency to  $1683\text{ cm}^{-1}$ , a value close to the Ar matrix value. Further increasing the field to  $0.0040$  au yields a proton-stretching frequency of  $1933\text{ cm}^{-1}$ , slightly greater than the experimental frequency in an  $\text{N}_2$  matrix.

At this point it should be noted that our modeling of matrix effects, in terms of a dipole induced reaction field, is complementary to very recent work by Sugarman et al.<sup>44</sup> In their study molecular dynamics simulations were used to investigate Ar matrix effects on the geometry of  $\text{CaF}_2$ . They concluded that changes in the structure of  $\text{CaF}_2$  were attributable to a reaction

field-induced dipole effect. Their work lends further support to the use of an external electric field to model the structural (and spectroscopic) effects induced by a matrix.

**Generalizations for the Cl–H–N Hydrogen Bond.** The plots shown in Figures 4 and 6 for  $\text{ClH:NH}_3$  and  $\text{ClH:N}(\text{CH}_3)_3$  demonstrate that external electric fields preferentially stabilize the proton-shared region of the potential energy surface relative to the region of the traditional hydrogen bond. This effect is most apparent in  $\text{ClH:NH}_3$ , since this complex has a traditional hydrogen-bonded structure at zero field, and moves to a proton-shared structure and then an ion-pair structure as the field strength increases. When the traditional and proton-shared regions are relatively close in energy on the zero-field surface, changes induced by an external field can have significant structural and spectroscopic consequences. At this point it is appropriate to generalize these effects, and to connect some of the observations made in this study to results of a previous investigation of selected  $\text{ClH:4-R-pyridine}$  complexes.<sup>11,12</sup>

Figure 8 presents one-dimensional normal coordinate displacement curves for the proton stretch obtained from the  $\text{ClH:NH}_3$  two-dimensional surfaces at each field strength. The highest-energy curve (solid curve) is the zero-field curve. The curves become displaced toward lower energy as the strength of the external field increases. The curves have been drawn so that the equilibrium structure on each curve is found at zero displacement along the normal coordinate axis. At zero field, the equilibrium structure of  $\text{ClH:NH}_3$  has a traditional hydrogen bond, with the proton-shared structure lying at higher energy in the region corresponding to the shoulder on the curve. As the field is turned on and increases from  $0.0010$  to  $0.0025$  and then to  $0.0040$  au, the energy difference between the minimum and the shoulder decreases as the structure assumes greater proton-shared character. At a field of  $0.0055$  au, the curve exhibits a broad, flat minimum, which suggests that it corresponds to a quasisymmetric hydrogen-bonded complex. That is, at this field strength the forces on the proton from Cl and N are approximately equal. The lowest-energy curve in Figure 8 corresponds to a field of  $0.0100$  au and shows that the equilibrium structure lies on the ion-pair side of quasisymmetric,

(44) Sugarman, R.; Wilson, M.; Madden, P. A. *Chem. Phys. Lett.* **1999**, *308*, 509.

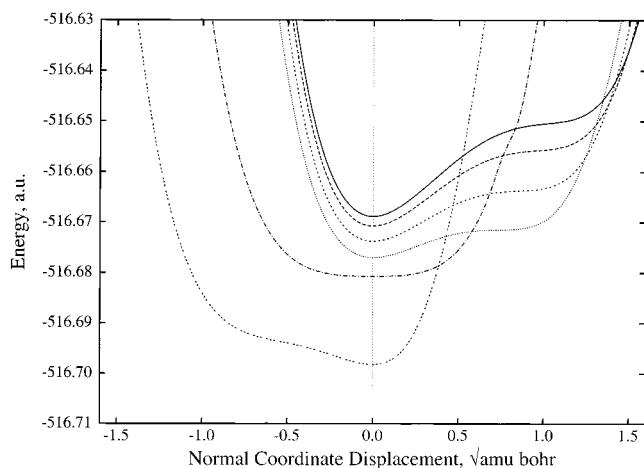


**Figure 8.** One-dimensional potential curves along the normal coordinate for the proton-stretching mode obtained from the two-dimensional surfaces as a function of field strength. The curve at highest energy (solid) is the zero-field curve. The remaining curves are obtained from surfaces with external fields of 0.0010, 0.0025, 0.0040, 0.0055, and 0.0100 au. The minima on these curves occur at lower energy as the field strength increases.

with the higher energy shoulder in the region of the traditional hydrogen-bonded complex. At very high fields the traditional hydrogen-bonded complex would lie significantly higher in energy relative to an equilibrium hydrogen-bonded ion pair.

Curves similar to the ones shown in Figure 8 can be found for ClH:pyridine in ref 39. In that work, three curves for the proton-stretching mode were presented. The first was the curve obtained from the normal coordinate displacement vector obtained from the computed harmonic spectrum. This curve exhibits a minimum corresponding to a traditional hydrogen-bonded structure, with a shoulder corresponding to a proton-shared structure. The energy difference between the traditional and proton-shared regions of the ClH:pyridine surface is less than it is for ClH:NH<sub>3</sub>. The second curve is a one-dimensional curve that was constructed to reproduce the experimental proton-stretching frequency for ClH:pyridine in an Ar matrix. The minimum on the curve is on the traditional side of quasisymmetric, and the energy gap between the minimum and the shoulder is reduced. In ref 39 a “correlated HCl distance” [ $R_{\text{cor}}(\text{HCl})$ ] was defined, which is the value of the HCl distance that correlates with the experimental proton-stretching frequency. The value of  $R_{\text{cor}}(\text{HCl})$  that corresponds to the second curve is 1.48 Å. This second ClH:pyridine curve is similar to the curves for ClH:NH<sub>3</sub> at external fields weaker than 0.0055 au in Figure 8. The third one-dimensional ClH:pyridine curve was constructed to reproduce the proton-stretching frequency of ClH:pyridine in an N<sub>2</sub> matrix. This curve has a minimum that lies on the ion-pair side of quasisymmetric, with  $R_{\text{cor}}(\text{HCl})$  equal to 1.60 Å. This curve resembles the ClH:NH<sub>3</sub> curve in Figure 8 that corresponds to a field of 0.0100 au. This comparison is not intended to imply what field strengths correspond to Ar or N<sub>2</sub> matrices, but to show that the application of an external electric field is a useful and relatively simple way to mimic the effects of the environment on hydrogen-bonded complexes.

Although obtained by a dramatically different, semiempirical approach, the “correlated HCl distance” from ref 39 appears to be related to the computed expectation values of the HCl distance in ClH:NH<sub>3</sub> complexes in the ground vibrational state as a function of field strength. These expectation values are reported in Table 3. As noted above, the one-dimensional curve from ref 39 for ClH:pyridine in Ar has  $R_{\text{cor}}(\text{HCl})$  equal to 1.48

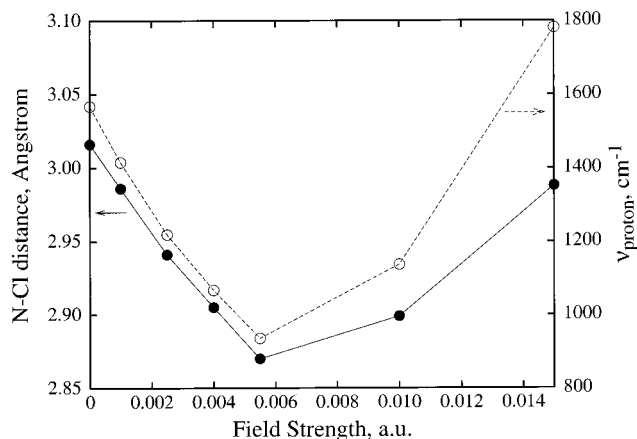


**Figure 9.** The expectation value of the Cl–N distance in the ground vibrational state and the proton-stretching frequency in ClH:NH<sub>3</sub> complexes as a function of field strength.

Å. The expectation values of the HCl distance in ClH:NH<sub>3</sub> complexes at fields of 0.0010, 0.0025, and 0.0040 au are 1.411, 1.448, and 1.495 Å, respectively. The value of  $R_{\text{cor}}(\text{HCl})$  for a quasisymmetric Cl–H–N hydrogen bond in ClH:pyridine was reported as 1.555 Å,<sup>39</sup> which is similar to the expectation value of the HCl distance of 1.546 Å for the curve in Figure 8 at a field strength of 0.0055 au. The curve at a field strength of 0.0100 au corresponds to a structure on the ion-pair side of quasisymmetric, and has a computed expectation value of the HCl distance of 1.692 Å. Curves at intermediate strength between 0.0055 and 0.0100 au would be expected to have expectation values of the HCl distance intermediate between 1.555 and 1.692 Å. The value of  $R_{\text{cor}}(\text{HCl})$  for the one-dimensional ClH:pyridine curve that lies on the ion-pair side of quasisymmetric is 1.60 Å.

Some structural and spectroscopic consequences of the application of external electric fields on the ClH:NH<sub>3</sub> complex can be seen in Figure 9, which shows plots of the proton-stretching frequency and the expectation value of the Cl–N distance versus the strength of the external electric field. A strong correlation between intermolecular distance and the proton-stretching frequency is evident from this figure. Both the proton-stretching frequency and the expectation value of the Cl–N distance decrease to a minimum at a field strength of approximately 0.0055 au, and then increase subsequently as the field strength increases. This behavior is consistent with the correlation found between computed equilibrium Cl–N distances and harmonic proton-stretching frequencies in a series of complexes formed between HCl and 4-substituted pyridines.<sup>11,12</sup> In this series, as the base strength of the substituted pyridine increases, the proton-stretching frequency and the intermolecular distance decrease, reaching a minimum for two complexes with proton-shared hydrogen bonds. These complexes have computed equilibrium intermolecular distances ( $R_e$ ) of 2.83 and 2.91 Å. The expectation values ( $R_0$ ) of the Cl–N distance in ClH:NH<sub>3</sub> at fields of 0.0040, 0.0055, and 0.0100 au are 2.975, 2.832, and 2.896 Å, respectively. Further increasing the base strength through substitution at the 4 position in pyridine leads to hydrogen-bonded ion pairs, with longer intermolecular distances and increased proton stretching frequencies which are perturbed N–H stretches. Thus, there is a correspondence between the changes in proton-stretching frequencies and intermolecular distances in ClH:NH<sub>3</sub> resulting from the application of external electric fields and changes induced internally in ClH:4-R-pyridine complexes by altering the basicity at the nitrogen through changing the substituent in the 4-position.

The observations made in this work and the similarities to findings in ref 39 are striking, particularly when it is noted that these two studies were performed not just at different levels of theory, but using different methods. In this work we have used variational methods whereas ref 39 followed a semiempirical approach. Despite these differences, both works strongly suggest that an HCl distance of approximately 1.55 Å is indicative of a quasisymmetric hydrogen bond, independent of the nature of the atom hydrogen bonded to Cl. This value of the HCl distance is also consistent with computed equilibrium HCl distances of 1.550 and 1.564 Å in the symmetric ion  $\text{ClHCl}^-$ , and 1.557 and 1.572 Å in  $\text{Cl}_2\text{H}_3^+$ , obtained at MP2/6-31+G(d,p) and MP2/ aug'-cc-pVDZ, respectively.

## Conclusions

Ab initio calculations have been carried out to examine the effects of external electric fields on X–H and X–N equilibrium distances, and on proton- and dimer-stretching frequencies in complexes with X–H–N hydrogen bonds, for X = Cl and Br. These calculations were carried out at MP2/aug'-cc-pVDZ for hydrogen-bonded complexes of HCl with  $\text{NH}_3$  and  $\text{N}(\text{CH}_3)_3$ , and at MP2/6-31+G(d,p) for the corresponding complexes with HBr. Anharmonic two-dimensional wave functions and proton- and dimer-stretching frequencies were computed from ab initio potential surfaces generated without and with external fields of varying strengths. The following conclusions are supported by the results of these calculations.

1. At zero-field, the HCl and HBr complexes with  $\text{NH}_3$  have equilibrium structures stabilized by traditional hydrogen bonds. The complex  $\text{ClH:N}(\text{CH}_3)_3$  has an equilibrium structure stabilized by a proton-shared hydrogen bond, while the equilibrium structure of  $\text{BrH:N}(\text{CH}_3)_3$  approaches that of a hydrogen-bonded ion pair.

2. External electric fields preferentially stabilize more polar structures, so that as the field strength increases, the equilibrium structure of a complex changes in the direction traditional, to proton-shared, to hydrogen-bonded ion pair. A quasisymmetric hydrogen bond is a special case of a proton-shared A–H–B hydrogen bond for which the forces on H exerted by A and B are equal.

3. The potential surfaces of these complexes are very anharmonic, either being broad and relatively flat around the global minimum or having a second region separated from the global minimum that can be accessed in either the  $\nu = 0$  or 1 state of the proton-stretching mode. An anharmonic treatment of the proton-stretching vibration is necessary to describe this vibration. A one-dimensional harmonic fit for the proton-stretching motion cannot describe the intricacies of these potential surfaces, so agreement between computed harmonic frequencies and experimental gas-phase or matrix frequencies should be viewed as fortuitous.

4. The computed zero-field anharmonic proton-stretching frequency should be compared with an experimental gas-phase frequency. However, the vibrational spectra of these complexes have been obtained only in low-temperature Ar and  $\text{N}_2$  matrices. Owing to the nature of the potential surfaces in these complexes, matrix effects may induce significant changes in equilibrium structures and vibrational frequencies, as summarized below.

- (a) For the  $\text{ClH:NH}_3$  complex, the computed gas-phase proton-stretching frequency is  $1567\text{ cm}^{-1}$ . As the field strength increases, the proton-stretching frequency decreases to a minimum of  $936\text{ cm}^{-1}$  at a field of 0.0055 au for a structure in which the hydrogen bond is close to quasisymmetric, and then subsequently increases with increasing field strength. The

changes in the intermolecular Cl–N distance parallel changes in the proton-stretching frequency, first decreasing to a minimum in the quasisymmetric hydrogen-bonded complex, and then increasing. The experimental proton-stretching frequencies of  $\text{ClH:NH}_3$  are  $1371$  and  $720\text{ cm}^{-1}$ , respectively, in Ar and  $\text{N}_2$ . Our calculations suggest that the equilibrium complex is on the traditional side of quasisymmetric in Ar and close to quasisymmetric in  $\text{N}_2$ .

- (b) For the  $\text{BrH:NH}_3$  complex, the computed gas-phase proton-stretching frequency is  $908\text{ cm}^{-1}$ . As the field strength increases, the proton-stretching frequency decreases to a minimum of  $809\text{ cm}^{-1}$  at a field of 0.0025 au for a structure in which the hydrogen bond is close to quasisymmetric, and then subsequently increases. The experimental Ar matrix proton-stretching frequency is  $729\text{ cm}^{-1}$ , while the value in an  $\text{N}_2$  matrix is  $1386\text{ cm}^{-1}$ . Our calculations suggest that in an Ar matrix, the equilibrium structure is close to quasisymmetric, while in  $\text{N}_2$  the equilibrium structure lies on the ion-pair side of quasisymmetric.

- (c) The zero-field equilibrium structure of  $\text{ClH:N}(\text{CH}_3)_3$  has a proton-shared hydrogen bond, while that of  $\text{BrH:N}(\text{CH}_3)_3$  approaches a hydrogen-bonded ion pair. The application of even weak electric fields on these two complexes increases Cl–N and Br–N distances, and computed anharmonic proton-stretching frequencies. For  $\text{ClH:N}(\text{CH}_3)_3$  the zero-field proton-stretching frequency of  $1135\text{ cm}^{-1}$  increases to 1222 and  $1476\text{ cm}^{-1}$  at field strengths of 0.0010 and 0.00400 au, respectively. The later value is close to the experimental proton-stretching frequency in Ar. It is anticipated that a further increase in field strength would produce an even greater proton-stretching frequency comparable to the frequency of  $1615\text{ cm}^{-1}$  observed in  $\text{N}_2$ . For  $\text{BrH:N}(\text{CH}_3)_3$ , the zero-field proton-stretching frequency is  $1593\text{ cm}^{-1}$ , while at field strengths of 0.0010 and 0.0040 au the computed frequencies increase to 1681 and  $1930\text{ cm}^{-1}$ . The experimental proton-stretching frequency in Ar is observed at  $1660\text{ cm}^{-1}$ , while in  $\text{N}_2$  a doublet is observed at 1890 and  $1872\text{ cm}^{-1}$ .

5. The field effects observed in this study provide insight into the influence that Ar and  $\text{N}_2$  matrices have in determining the proton-stretching frequencies in hydrogen-bonded complexes. If the equilibrium structure at zero field corresponds to a traditional hydrogen-bonded complex, or to a proton-shared structure that lies on the traditional side of quasisymmetric, application of an external field will first decrease the proton-stretching frequency, and then subsequently increase it as the structure moves to the ion-pair side of quasisymmetric. However, if the zero-field structure is quasisymmetric or on the ion-pair side of quasisymmetric, then application of an external field of any strength will lead to an increase in the proton-stretching frequency. Thus, the apparently opposing effects of Ar and  $\text{N}_2$  matrices on related complexes such as  $\text{ClH:NH}_3$  and  $\text{ClH:N}(\text{CH}_3)_3$  can be understood.

6. For complexes with Cl–H–B hydrogen bonds, it appears that a quasisymmetric hydrogen bond has a ClH distance of about 1.55 Å, independent of the nature of B.

7. The use of zero-point vibrational energy corrections based on harmonic proton-stretching frequencies can lead to relatively large errors in binding enthalpies in some complexes, as found for  $\text{BrH:NH}_3$  and  $\text{ClH:N}(\text{CH}_3)_3$ . The former complex with a traditional hydrogen bond can access the proton-shared region of the surface in the  $\nu = 0$  state, while the latter complex is found in a broad and relatively flat region of the surface associated with a proton-shared hydrogen bond. In both cases, the harmonic zero-point vibrational energy is too high.



**Acknowledgment.** The authors acknowledge support of this work from the National Science Foundation through grant CHE-9873815. The calculations reported were done using the computing facilities at the Ohio Supercomputer Center, Cambridge University, and the University of Sydney. The authors

wish to thank Dr. Jeff Reimers for helpful suggestions. J.E.D.B. thanks the School of Chemistry at the University of Sydney for hospitality during a Visiting Professorship.

JA993981S